doi:10.1093/brain/awz381 BRAIN 2020: 143; 191–209 | 191

BRAIN
A JOURNAL OF NEUROLOGY

Alzheimer-like amyloid and tau alterations associated with cognitive deficit in temporal lobe epilepsy

Sarah Gourmaud,[1] Haochang Shou,[2] David J. Irwin,[1,3] Kimberly Sansalone,[1] Leah M. Jacobs,[1] Timothy H. Lucas,[4] Eric D. Marsh,[1,5] Kathryn A. Davis,[1] Frances E. Jensen,[1,*] and Delia M. Talos[1,*]

*These authors contributed equally to this work.

Temporal lobe epilepsy represents a major cause of drug-resistant epilepsy. Cognitive impairment is a frequent comorbidity, but the mechanisms are not fully elucidated. We hypothesized that the cognitive impairment in drug-resistant temporal lobe epilepsy could be due to perturbations of amyloid and tau signalling pathways related to activation of stress kinases, similar to those observed in Alzheimer's disease. We examined these pathways, as well as amyloid-β and tau pathologies in the hippocampus and temporal lobe cortex of drug-resistant temporal lobe epilepsy patients who underwent temporal lobe resection (n = 19), in comparison with age- and region-matched samples from neurologically normal autopsy cases (n = 22). Post-mortem temporal cortex samples from Alzheimer's disease patients (n = 9) were used as positive controls to validate many of the neurodegeneration-related antibodies. Western blot and immunohistochemical analysis of tissue from temporal lobe epilepsy cases revealed increased phosphorylation of full-length amyloid precursor protein and its associated neurotoxic cleavage product amyloid-β*56. Pathological phosphorylation of two distinct tau species was also increased in both regions, but increases in amyloid-$\beta_{1\text{-}42}$ peptide, the main component of amyloid plaques, were restricted to the hippocampus. Furthermore, several major stress kinases involved in the development of Alzheimer's disease pathology were significantly activated in temporal lobe epilepsy brain samples, including the c-Jun N-terminal kinase and the protein kinase R-like endoplasmic reticulum kinase. In temporal lobe epilepsy cases, hippocampal levels of phosphorylated amyloid precursor protein, its pro-amyloidogenic processing enzyme beta-site amyloid precursor protein cleaving enzyme 1, and both total and hyperphosphorylated tau expression, correlated with impaired preoperative executive function. Our study suggests that neurodegenerative and stress-related processes common to those observed in Alzheimer's disease may contribute to cognitive impairment in drug-resistant temporal lobe epilepsy. In particular, we identified several stress pathways that may represent potential novel therapeutic targets.

1 Department of Neurology, Perelman School of Medicine, University of Pennsylvania, Philadelphia, PA, USA
2 Department of Biostatistics, Epidemiology and Informatics, Perelman School of Medicine, University of Pennsylvania, Philadelphia, PA, USA
3 Penn Frontotemporal Degeneration Center, University of Pennsylvania, Philadelphia, PA, USA
4 Department of Neurosurgery, University of Pennsylvania, Perelman School of Medicine, Philadelphia, PA, USA
5 Division of Child Neurology, Children's Hospital of Philadelphia, Philadelphia, PA, USA

Correspondence to: Delia M. Talos, MD
415 Curie Boulevard
263 Clinical Research Building
Philadelphia, PA, 19104, USA
E-mail: talosd@pennmedicine.upenn.edu

Received March 15, 2019. Revised October 8, 2019. Accepted October 17, 2019. Advance Access publication December 13, 2019

Correspondence may also be addressed to: Frances E. Jensen, MD
3400 Spruce Street
Hospital of the University of Pennsylvania, Dulles 3
Philadelphia, PA 19104, USA
E-mail: frances.jensen@pennmedicine.upenn.edu

Keywords: temporal lobe epilepsy; cognition; beta-amyloid; tau; stress-related kinases

Abbreviations: eIF2α = eukaryotic initiation factor 2α; GSK-3β = glycogen synthase kinase 3β; JNK = c-Jun N-terminal kinase; mTOR = mechanistic target of rapamycin; p70S6K = p70 ribosomal protein S6 kinase; PERK = protein kinase R-like endoplasmic reticulum kinase; PP2A = protein phosphatase 2A; p-tau = hyperphosphorylated tau; TLE = temporal lobe epilepsy

Introduction

Temporal lobe epilepsy (TLE) is one of the most common forms of focal epilepsy in adolescents and adults (Tellez-Zenteno and Hernandez-Ronquillo, 2012). Approximately one-third of patients are drug-resistant, for which surgical resection is a potentially curative treatment (Hernandez-Ronquillo *et al.*, 2016; Asadi-Pooya *et al.*, 2017). Hippocampal sclerosis is the most common histopathological finding in surgical tissue from patients with TLE (Blumcke *et al.*, 2017). Cognitive comorbidities in TLE can be significant and not only limited to memory deficits, but can also encompass a wide range of cognitive domains including language, executive function, attention and processing speed (Jensen, 2011; Elverman *et al.*, 2019). Cognitive disability is greater in patients with drug-resistant epilepsy and frequent interictal spikes, suggesting direct effects of the epileptogenic process (Kleen *et al.*, 2013; Gelinas *et al.*, 2016; Ung *et al.*, 2017). Alternatively, cognitive impairment may already be present at disease onset or even before seizures manifest (Taylor *et al.*, 2010; Osler *et al.*, 2018), implying shared underlying mechanisms. Given that mechanisms for cognitive impairment in TLE are unknown, treatment options for cognitive dysfunction in epilepsy are limited.

Several lines of evidence suggest that the same mechanisms associated with pathological brain ageing and neurodegeneration might also be responsible for cognitive dysfunction in patients with epilepsy. Strikingly, patients with therapy-resistant chronic epilepsy show imaging characteristics of advanced brain ageing (Pardoe *et al.*, 2017), increased amyloid-β_{42} burden (Joutsa *et al.*, 2017) and accelerated ventricular expansion (Dabbs *et al.*, 2012), similar to characteristics seen in neurodegenerative cognitive disorders such as Alzheimer's disease.

The cellular and molecular basis for cognitive decline in Alzheimer's disease is the progressive accumulation of hyperphosphorylated tau (p-tau) protein in neurofibrillary tangles, the production of neurotoxic amyloid-β_{42} species, including soluble amyloid-β*56, and the extracellular amyloid-β_{42} accumulation into insoluble amyloid plaques (Cleary *et al.*, 2005; Di *et al.*, 2016). Amyloid-β_{42} is produced via amyloidogenic processing of the amyloid precursor protein (APP) by β-site amyloid precursor protein cleaving enzyme 1 (BACE1) and γ-secretase (O'Brien and Wong, 2011) (Fig. 1). Tau phosphorylation, a prerequisite for tau aggregation and toxicity, is regulated by several protein kinases and phosphatases, including c-Jun N-terminal kinase (JNK), p70 ribosomal protein S6 kinase (p70S6K), glycogen synthase kinase 3β (GSK-3β), cyclin-dependent kinase 5 (CDK5) and protein phosphatase 2A (PP2A) (Martin *et al.*, 2013; Wang *et al.*, 2013).

Neurodegenerative processes including increased expression of APP and occasional presence of amyloid plaques and neurofibrillary tangles have been observed in brain specimens from drug-resistant epilepsy cases, including patients with TLE, tuberous sclerosis complex, focal cortical dysplasia and glioneuronal tumours (Mackenzie and Miller, 1994; Sheng *et al.*, 1994; Thom *et al.*, 2011; Iyer *et al.*, 2014; Sima *et al.*, 2014; Prabowo *et al.*, 2015; Puvenna *et al.*, 2016; Tai *et al.*, 2016). APP and amyloid-β_{42} increases have also been found in other diseases associated with seizures and cognitive impairment, such as Down syndrome and fragile X syndrome (Westmark *et al.*, 2016; Perez *et al.*, 2019).

These associations raise the possibility that hyperexcitable networks may trigger neurodegenerative changes and that activity-dependent signalling may play a role. One such link may be the mechanistic target of rapamycin (mTOR), which has been implicated in epileptogenesis and its cognitive comorbidities (Zeng *et al.*, 2009; Huang *et al.*, 2010; Talos *et al.*, 2012; Lippman-Bell *et al.*, 2013). The mTOR pathway is profoundly dysregulated in human TLE (Talos *et al.*, 2018) and Alzheimer's disease (Sun *et al.*, 2014). mTOR is involved in amyloid-β_{42} generation and clearance, tau protein synthesis and tau phosphorylation (Pei *et al.*, 2006; Caccamo *et al.*, 2010, 2013, 2015; Tang *et al.*, 2015) (Fig. 1). The mTOR pathway is also linked to endoplasmic reticulum stress (Di Nardo *et al.*, 2009; Appenzeller-Herzog and Hall, 2012), which has been implicated in early stages of Alzheimer's disease pathology (O'Connor *et al.*, 2008; Hoozemans *et al.*, 2012; Devi and Ohno, 2014) and observed in several acute seizure models (Carnevalli *et al.*, 2006; Torres-Peraza *et al.*, 2013; Chen *et al.*, 2014), but less studied in human TLE.

The goal of the present study was to build upon existing evidence for a relationship between amyloid and tau pathologies, cognitive dysfunction and epileptogenesis in drug-resistant TLE and to further elucidate specific signalling elements involved. We hypothesized that uncontrolled seizures, mTOR activation and cellular stress may synergize to

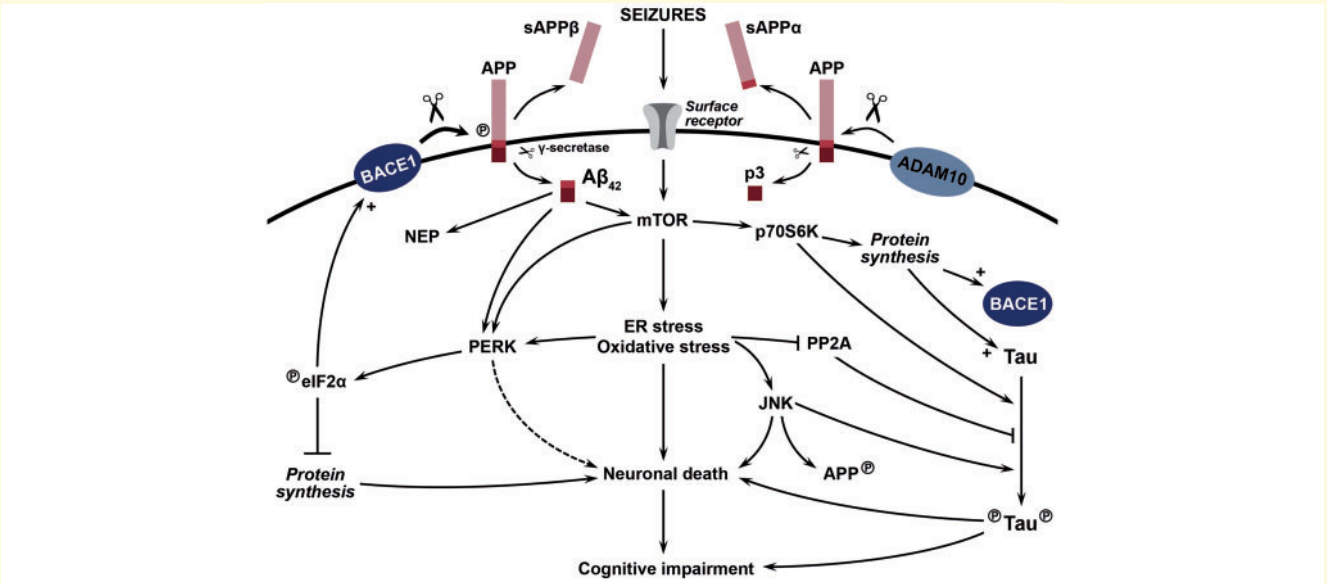

Figure 1 Hypotheses for the accumulation of amyloid-β_{42} and tau pathology linked to cognitive impairment and epileptogenesis in TLE. Following seizures, activation of surface receptors, including excitatory neurotransmitter receptors, activates the mTOR pathway leading to an increase in endoplasmic reticulum (ER) stress and oxidative stress. Chronic activation of cell stress pathways leads to neuronal death and subsequent cognitive impairment. ER stress activates PERK, which in turn phosphorylates and activates eIF2α, causing a general inhibition of protein synthesis leading to neuronal death. At the same time, phosphorylated (circled P) eIF2α de-represses the translation of *BACE1* mRNA, increasing the amyloidogenic processing of APP, a process further augmented following APP phosphorylation (circled P). The amyloidogenic processing of APP (represented by large scissors) by β-secretase BACE1 results in the release of soluble APPβ (sAPPβ), while the subsequent cleavage of the remaining transmembrane APP portion (represented by small scissors) by γ-secretase generates the amyloid-β_{42} peptide. In a similar fashion, the non-amyloidogenic processing of APP by α-secretase ADAM10 and γ-secretase results in the release of soluble APPα (sAPPα) and the p3 peptide. While also further inducing mTOR activity, ER stress, and oxidative stress, amyloid-β_{42} peptides increase the expression of neprilysin (NEP), a major amyloid-β_{42}-degrading enzyme participating in amyloid-β_{42} clearance. The ribosomal protein kinase p70S6K, a downstream target of activated mTOR, induces the synthesis of tau and BACE1 proteins and directly phosphorylates tau (circled P). Cellular stress also leads to activation of pro-apoptotic JNK, in addition to inhibiting PP2A activity. PP2A is a major tau phosphatase and its activation leads to decreased tau phosphorylation. JNK phosphorylates APP and tau protein (circled P), and induces *BACE1* transcription (not shown).

increase APP, tau, and BACE1 levels to accelerate amyloid-β_{42} production and tau pathology, and thus cause neuronal dysfunction and cognitive impairment in the setting of TLE (Fig. 1). These links have not yet been established, and if identified could reveal potential novel therapeutic targets for management of seizures and their cognitive consequences.

Materials and methods

Study population

The TLE group consisted of 19 patients (9 males/10 females) with drug-resistant epilepsy who underwent anterior temporal lobe resections at the Hospital of the University of Pennsylvania, Philadelphia, PA (n = 14), the Children's Hospital of Philadelphia (n = 2) and the Boston Children's Hospital, MA (n = 3), as part of their epilepsy treatment. Written informed consent for the use of brain tissue and review of medical records was obtained from all patients before surgery according to the Declaration of Helsinki. The study was approved by the Institutional Review Board at each institution. The mean age at surgery was 29 years (range 10–56). The majority of cases (63.2%; n = 12) presented with hippocampal sclerosis (Blumcke *et al.*, 2013). A subset of patients (26.3%; n = 5) were diagnosed with dual pathology, defined by the presence of a primary lesion within the ipsilateral temporal lobe or hemisphere (Blumcke *et al.*, 2011), and consisting of focal cortical dysplasia type IIa (n = 2), dysembryoplastic neuroepithelial tumour (n = 1), periventricular heterotopia (n = 1) and leptomeningeal vascular malformation (n = 1) (Supplementary Table 1).

The control cases (n = 22; 16 males/6 females) were obtained from the NIH NeuroBioBank and the Institute on Aging, Center for Neurodegenerative Disease Research (IOA-CNDR) of the University of Pennsylvania (Supplementary Table 2). All samples were collected post-mortem. The mean age at death was 37.7 years (range 4–67). All control cases were diagnosed as histologically normal and none of the cases had a known history of epilepsy, dementia, or any other neurological or psychiatric illness. All control patients died of non-neurological causes. In addition, post-mortem temporal lobe specimens from Alzheimer's disease patients (n = 9; four males/five females) were included as a positive control group. Samples were obtained from the IOA-CNDR. The mean age at death was 77.9 years (range 64–91) (Supplementary Table 2). Alzheimer's disease diagnosis was established based on clinical history, neurological and neuropsychological assessment, and

neuropathological staging of related changes (amyloid-β plaques, Braak stage, neuritic plaques) (McKhann *et al.*, 2011). All patients had sporadic Alzheimer's disease and presented advanced pathology (Braak 5–6 and Thal 5), but no reported seizure history.

Research involving human participants

All procedures performed in studies involving human participants were in accordance with the ethical standards of the institutional and/or national research committee and with the 1964 Helsinki declaration and its later amendments or comparable ethical standards. This report does not contain any studies with animals performed by any of the authors. Informed consent was obtained from all individual participants included in the study.

Neuropsychological assessment

All TLE patients underwent routine pre-surgical neuropsychological examination, including IQ measurements and assessment of memory (episodic verbal memory and episodic visuospatial memory), language and executive function. We only used the adult cognitive data for correlation studies (n = 14), given the lack of equivalence between the adult and paediatric cognitive datasets. No correlative analyses were performed in Alzheimer's disease, as cognitive assessment was not uniform and performed over variable periods prior to death. Test percentile scores, based on their respective demographic norms (age, gender, etc.), were converted into z-scores. Detailed cognitive data for adult TLE cases are presented in Supplementary Table 3 and the Supplementary material, methods section.

Protein analysis and immunohistochemistry

Frozen samples from anatomically comparable regions containing similar amounts of white and grey matter in all subjects, were homogenized and used for western blot analysis. Formalin-fixed paraffin-embedded tissue blocks were sectioned at 6 µm and subjected to either diaminobenzidine or fluorescence immunohistochemistry procedures. Additional immunohistochemistry was carried out on 4% paraformaldehyde-fixed (20–µm sections) or isotonic 70% ethanol (6–µm sections) to confirm antigen preservation and rule out potential artefacts due to formalin fixation. All samples were processed using standard protocols and solutions (Gourmaud *et al.*, 2015; Talos *et al.*, 2018). Primary antibody characterization, including previous studies demonstrating their specificity, can be found in the Supplementary material, methods section. Specificity was further determined by western blotting (Supplementary Fig. 1).

Statistical analysis

Western blot data were expressed as fold-change or percentage relative to age-adjusted controls. Markers were first screened by comparing group means using two-tailed Student t-test (normal distribution) or Mann-Whitney test (skewed distribution) with GraphPad Prism 7 (San Diego, CA). The D'Agostino-Pearson test was used to assess the normality of each distribution (Prism 7). Detailed statistical data, with unadjusted P-values, group sizes, distribution normality, and confidence intervals are presented in Supplementary Table 4. Merged group data are illustrated as box-and-whisker plots indicating minimum and maximum, first and third quartile, and median values. Relative protein levels for individual markers in TLE and control groups were further analysed via multivariate linear regression models adjusting for age at surgery and gender: Model 1 comparing epilepsy with controls, Model 2 stratifying epilepsy cases by the presence or absence of hippocampal sclerosis, and Model 3 stratifying by seizure focus location (R Core Team, Vienna, Austria). Wald tests of the regression coefficients were used to determine significance and multiple comparisons were corrected with Benjamini and Hochberg false discovery rate method for multiple testing (22 markers and three models) (R software). Adjusted and corrected P-values, with beta coefficients, are presented in Supplementary Table 5. Partial correlation analyses of pairwise western blot markers were adjusted for the effect of gender, age at surgery and disease duration (Partial correlation, R software). As cognitive test results were already expressed as z-scores following age and gender correction, we did not further adjust for covariates and used Pearson correlation coefficients (Prism 7) to examine potential associations between cognitive function and protein markers. Regression analyses were also performed to determine the effect of post-mortem interval on individual protein expression levels. Test results were considered significant at $P \leqslant 0.05$.

Data availability

The data that support the findings of this study are available from the corresponding authors upon reasonable request.

Results

Increased APP expression and phosphorylation in human temporal lobe epilepsy

Western blot analysis using an antibody that specifically recognizes amino acids 66–81 of APP (clone 22C11; Supplementary Fig. 1A, top) (Hilbich *et al.*, 1993), demonstrated a significant increase in full-length APP expression in TLE hippocampus (172% of controls, $P < 0.01$), but no change in TLE cortex (Fig. 2A). As the phosphorylation of APP at threonine 668 (Thr668) facilitates APP amyloidogenic processing and Alzheimer's disease pathology (Lee *et al.*, 2003), we next analysed the expression of phosphorylated APP (Thr668) (pAPP; antibody clone D90B8; Supplementary Fig. 1A, bottom) and found increased levels in both TLE hippocampus (249% of controls, $P < 0.01$) and temporal cortex (237% of controls, $P < 0.0001$) (Fig. 2B). The observed group differences for APP and pAPP (Supplementary Table 4) remained statistically significant in both brain regions after adjusting for age at surgery and gender, and correcting for the number of analysed markers

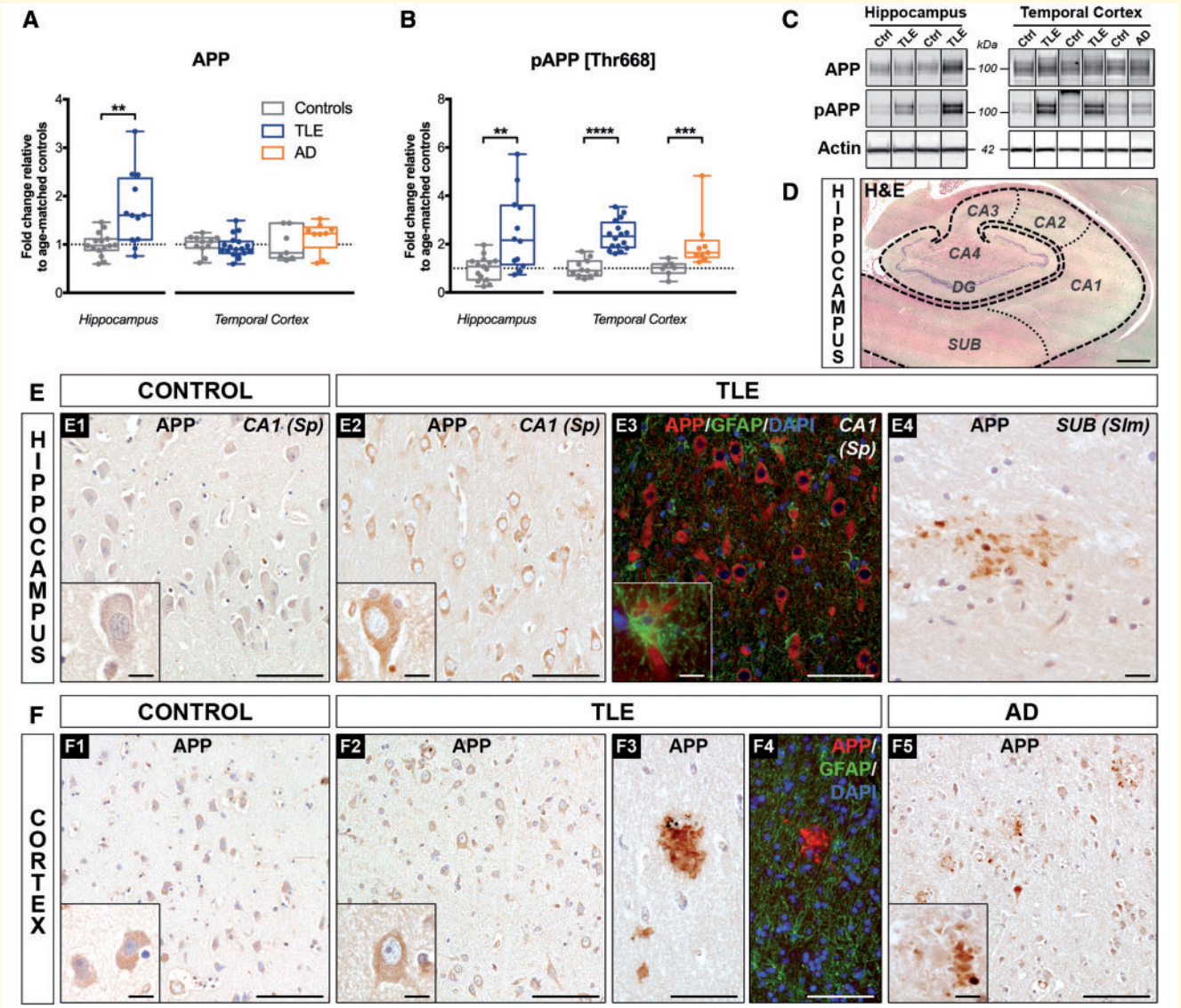

Figure 2 Increased expression and phosphorylation of APP in human drug-resistant TLE. (**A** and **B**) Western blot quantification of (**A**) total APP and (**B**) phospho-APP [Thr668] in the hippocampus and temporal cortex from TLE, Alzheimer's disease and control patients. Data are represented as box-and-whisker plots showing the minimum value, the first quartile, the median, the third quartile, and the maximum value. Each group is compared to its respective age-matched control group using two-tailed Student *t*-test (normal distribution) or Mann-Whitney test (skewed distribution). $^{*}P < 0.05$, $^{**}P < 0.01$, $^{****}P < 0.0001$. Detailed statistical data are provided in Supplementary Table 4. (**C**) Representative western blot images showing non-adjacent bands originating from the same blot. (**D**) Representative hippocampal section from a 37-year-old control subject (Ctrl 11) stained with haematoxylin and eosin (H&E) indicating the subfields imaged for staining illustrations: subiculum (SUB), Cornu Ammonis (CA1 to CA4), and dentate gyrus (DG) with its discernible granule cell layer. (**E**) Photomicrographs showing the hippocampal CA1 pyramidal cell layer from (**E1**) a 37-year-old control subject (Ctrl 11); (**E2**) a 29-year-old TLE patient with hippocampal sclerosis type III (TLE 12), (**E3**) the CA1 pyramidal cell layer, and (**E4**) the molecular layer of the SUB region from a 20-year-old TLE patient with hippocampal sclerosis type I (TLE 6); each immunolabelled with APP antibody (clone 22C11) or co-immunolabelled with APP (red), astrocytic marker GFAP (green), and nuclear stain DAPI (blue). Images show enhanced intra-neuronal APP labelling in the TLE hippocampus (**E2**) relative to control (**E1**), no detectable APP expression in the astrocytes (**E3**), and the presence of occasional extracellular APP depositions suggestive of diffuse amyloid plaques (**E4**). Note the similarities between the diaminobenzidine (**E2**) and the immunofluorescence (**E3**) APP signal. (**F**) Representative images of the temporal cortex from (**F1**) a 55-year-old control subject (Ctrl 15), (**F2**) a 29-year-old, (**F3**) a 24-year-old, and (**F4**) a 38-year-old TLE patient (TLE 12, TLE 7 and TLE 14, respectively), alongside with temporal cortex images from (**F5**) a 65-year-old Alzheimer's disease patient (AD 8); each labelled with APP (22C11) or co-immunolabelled with APP (red), GFAP (green), and DAPI (blue). Images demonstrate no apparent differences in neuronal APP expression between TLE (**F2**) and control cortex (**F1**), despite the presence of occasional amyloid plaque-like extracellular deposits (**F3** and **F4**), similar to what is observed in the Alzheimer's disease case (**F5**). Diaminobenzidine (**F3**) and immunofluorescence (**F4**) APP labelling showing comparable signal patterns and the lack of APP co-localization with GFAP in the TLE cases (**F4**). Scale bars = 1000 μm in **D**, 100 μm in **E1**–**3**, **F1**–**5**; 10 μm in **E4**; *insets* = 10 μm.

(Supplementary Table 5). Alzheimer's disease temporal cortex showed a similar increase in pAPP expression (204% of controls, $P < 0.001$), as expected, but no change in full-length APP levels (Kirouac *et al.*, 2017).

Immunohistochemistry for APP protein revealed increased intraneuronal staining in TLE samples compared to controls [Fig. 2E(1–2) and F(1–2)], as previously described (Sheng *et al.*, 1994; Sima *et al.*, 2014). In the TLE hippocampus, APP was mostly expressed in the subiculum and CA1–CA4 pyramidal cell layer [Fig. 2E(2–4) and Supplementary Fig. 2A]. Double labelling with GFAP demonstrated little to no APP expression in astrocytes [Fig. 2E(3)]. APP was occasionally seen in endothelial cells (data not shown). In the temporal cortex, neuronal APP staining was observed throughout all layers [Fig. 2F(2)]. In 3 of 11 TLE cases (27%), we detected extracellular APP depositions with morphological characteristics suggestive of diffuse amyloid plaques [Fig. 2E(4) and F(3–4)], distinct from the fibrillar plaques seen in Alzheimer's disease cases [Fig. 2F(5)]. The plaque-like deposits in TLE samples were rather rare (n = 1–3 plaques/section) and occurred in the hippocampus, predominantly in the subiculum, as well as in the temporal cortex, mostly in the upper layers (Supplementary Fig. 2A).

Upregulation of amyloidogenic APP cleavage products in temporal lobe epilepsy

Given the elevated APP levels, we next assessed the expression of several APP cleavage products resulting from non-amyloidogenic [soluble (s)APPα] or amyloidogenic (sAPPβ and amyloid-β_{42} peptide) processing (Supplementary Fig. 1B) (O'Brien and Wong, 2011). SAPPα expression was increased in TLE hippocampus (147% of controls, $P < 0.05$), but not in temporal cortex (Fig. 3A). However, the adjustment for covariates and the correction for multiple testing rendered hippocampal sAPPα expression not significant. SAPPβ protein was not significantly changed in TLE (Fig. 3B), most likely due to rapid degradation (Morales-Corraliza *et al.*, 2009). Western blot analysis for amyloid-β_{42} (antibody clone MOAB-2; Fig. 3C–E and Supplementary Fig. 1C) (Youmans *et al.*, 2012) revealed three main species: a band at 56 kDa (dodecameric non-fibrillar amyloid-β^*56), a band at 25 kDa (amyloid-β_{42} fibrillar hexamers), and a smear ranging from 2 to 15 kDa (amyloid-β_{42} monomers and fibrillar dimers). The expression of amyloid-β^*56 (Fig. 3C) was significantly upregulated in TLE hippocampus (253% of controls, $P < 0.0001$) and temporal cortex (270% of controls, $P < 0.001$), while amyloid-β_{42} (merged data obtained for hexamers, dimers and monomers) was upregulated exclusively in the hippocampus (239% of controls, $P < 0.01$) (Fig. 3D). Both amyloid-β^*56 and amyloid-β_{42} remained statistically significant after adjusting for covariates and correcting for the number of markers (Supplementary Tables 4 and 5). Similarly, in Alzheimer's disease temporal cortex, sAPPα and sAPPβ expression was not significantly altered, while both amyloid-β^*56 and amyloid-β_{42} levels were significantly increased (211% of controls, $P < 0.01$ and 341% of controls, $P < 0.01$, respectively).

Immunohistochemistry for amyloid-β_{42} revealed punctate amyloid-β_{42} immunoreactivity in both neurons and endothelial cells in the TLE hippocampus (Fig. 3G) and temporal cortex (Fig. 3H), as opposed to controls where the expression was low or undetectable. In the hippocampus, intraneuronal amyloid-β_{42} was found mostly in the CA pyramidal cells, while intra-endothelial amyloid-β_{42} was found in all regions, including the CA1 stratum lacunosum moleculare, as illustrated in Fig. 3G. In the TLE temporal cortex, amyloid-β_{42} expression was observed throughout all layers, presenting as intraneuronal, intra-endothelial and extracellular granular labelling, but was much less robust compared to Alzheimer's disease tissue showing strong extracellular amyloid-β_{42} immunoreactivity consistent with fibrillar, compact, and cored amyloid plaques (Fig. 3H).

To assess whether upregulation of amyloid-β_{42} in TLE could be related to an impairment of amyloid clearance, as previously observed in Alzheimer's disease (Kurz and Perneczky, 2011), we quantified the expression of neprilysin, the main amyloid-β_{42} degrading enzyme. Neprilysin was significantly increased in TLE hippocampus (330% of controls, $P < 0.01$), but not in temporal cortex (Supplementary Fig. 3), although the difference was no longer significant after adjustment and correction (Supplementary Tables 4 and 5). Neprilysin expression was unchanged in Alzheimer's disease temporal cortex.

Differential expression of APP processing enzymes ADAM10 and BACE1 in temporal lobe epilepsy

Since we found an upregulation of amyloidogenic APP cleavage products in TLE, we then analysed the expression of the main APP processing enzymes ADAM10 (non-amyloidogenic processing) and BACE1 (amyloidogenic processing) (O'Brien and Wong, 2011). By western blotting, we found no change in ADAM10 expression in TLE hippocampus and temporal cortex (Fig. 4A), in contrast to BACE1 expression, which was significantly increased in both brain regions (159% of controls, $P < 0.05$ in the hippocampus and 189% of controls, $P < 0.0001$ in the temporal cortex). After adjustment and correction, BACE1 expression remained significantly increased only in the temporal cortex (Supplementary Tables 4 and 5). A similar pattern was observed in Alzheimer's disease cases, where there was no change in ADAM10, but a significant increase in BACE1 expression (181% of controls, $P < 0.01$) (Fig. 4B).

Immunohistochemistry analysis for ADAM10 and BACE1 revealed a predominant intraneuronal expression pattern in both brain regions, most prominent in the large pyramidal

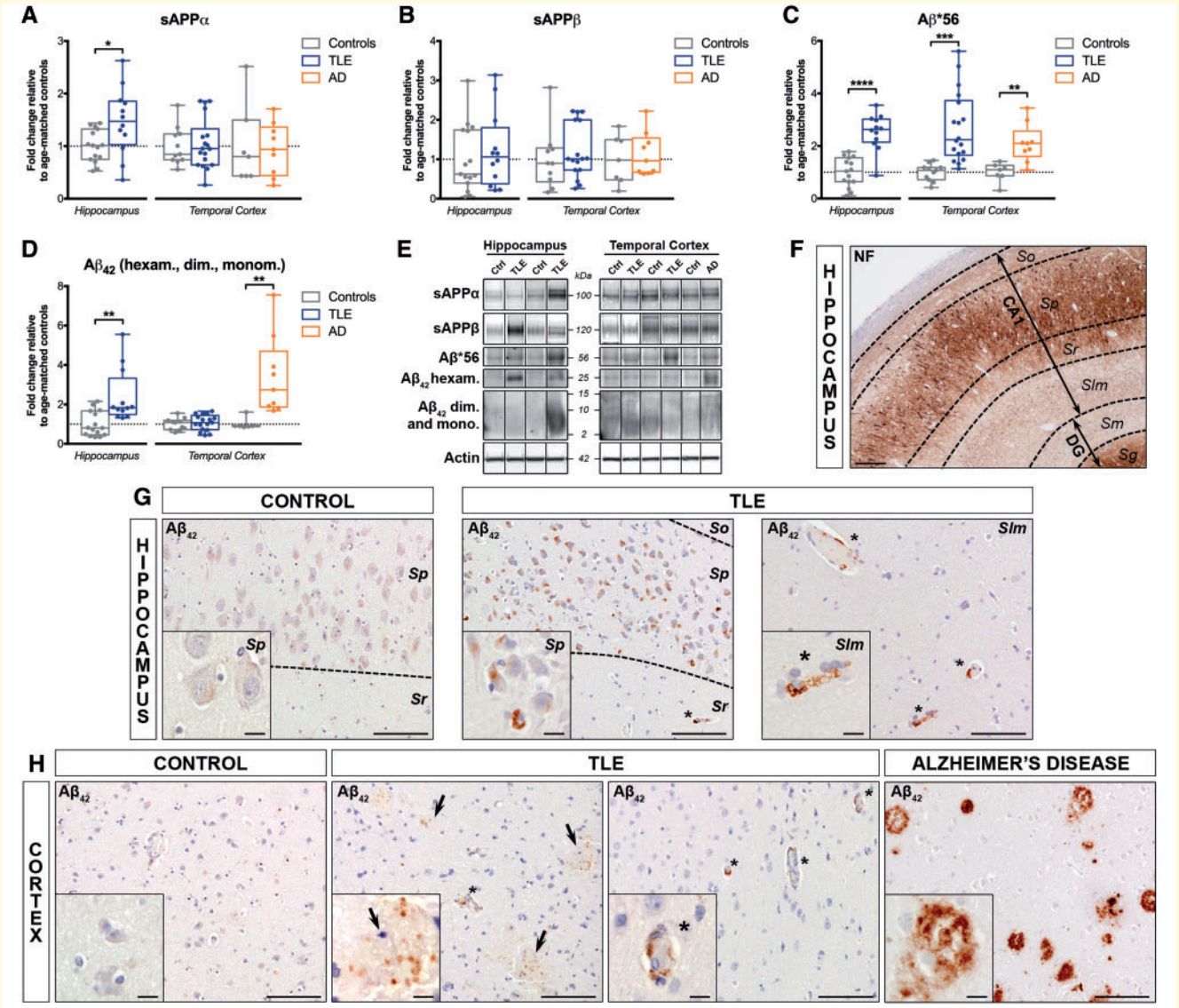

Figure 3 Increased expression of sAPPα, amyloid-β*56 and amyloid-β42 in human drug-resistant TLE. (**A**–**D**) Western blot quantification of (**A**) sAPPα, (**B**) sAPPβ, (**C**) amyloid-β*56, and (**D**) amyloid-β42 (average of amyloid-β42 hexamers, dimers and monomers) in the hippocampus and temporal cortex of TLE, Alzheimer's disease (AD) and control patients. Box-and-whisker plots display the minimum value, the first quartile, the median, the third quartile, and the maximum value. Each group is compared to its respective age-matched control group using two-tailed Student *t*-test (normal distribution) or Mann-Whitney test (skewed distribution). $^{*}P < 0.05$, $^{**}P < 0.01$, $^{***}P < 0.001$, $^{****}P < 0.0001$. Detailed statistical data are provided in Supplementary Table 4. (**E**) Representative western blot bands for the box-and-whisker plot graphs shown in **A**–**D**. Each lane shows non-adjacent bands from the same hippocampus or cortex blot. (**F**) Representative hippocampal section from a 38-year-old TLE patient without hippocampal sclerosis (TLE 14) stained for neurofilaments (NF) indicating the cellular layers for individual regions: stratum oriens (So), stratum pyramidale (Sp), stratum radiatum (Sr), and stratum lacunosum moleculare (Slm) for subiculum (SUB) and CA1–4, and stratum moleculare (Sm), stratum granulare (Sg) and hilus (not shown) for dentate gyrus (DG). (**G**) Representative images of the hippocampal CA1 from a 55-year-old control subject (Ctrl 15) and from a 38-year-old TLE patient without hippocampal sclerosis (TLE 14) labelled with amyloid-β42 antibody (clone MOAB-2), showing more frequent intracellular amyloid-β42 accumulation in neuronal cell bodies and endothelial cells of blood vessels (asterisks) in the TLE case versus control. (**H**, *middle left*) Temporal lobe cortex from the same cases shown in **G** immunohistochemically labelled with amyloid-β42 (MOAB-2), demonstrating occasional intracellular amyloid-β42 expression in endothelial cells (asterisks), as well as granular extracellular amyloid-β42 immunoreactivity (arrows) in TLE patient samples, but not in the control case. (**H**, *right*) Representative images of temporal lobe cortex from a 70-year-old Alzheimer's disease patient (AD 3) labelled with the same anti-amyloid-β42 monoclonal antibody as in **G** and **H** showing robust accumulation of amyloid-β42 in fibrillar, compact and cored amyloid plaques. Scale bars = 200 μm in **F**, 100 μm in **G** and **H**; *insets* = 10 μm. dim. = dimers; hexam. = hexamers; mono. = monomers.

neurons of the subiculum and CA1–4 and in the granule cells of the dentate gyrus. ADAM10 immunoreactivity in TLE was comparable to controls both in the hippocampus (Fig. 4D, top) and in the temporal cortex (not shown). BACE1 immunoreactivity appeared stronger in both TLE hippocampus (Fig. 4D, bottom) and temporal cortex (not shown) compared to controls. Alzheimer's disease temporal cortex showed low ADAM10 expression (Fig. 4E, top), but robust BACE1 labelling around fibrillar amyloid plaques (Fig. 4E, bottom).

Increased expression of tau and hyperphosphorylated tau in human temporal lobe epilepsy

As we found evidence for enhanced amyloidogenic APP processing in TLE, we next investigated whether this was accompanied by significant tau pathology, as seen in Alzheimer's disease patients (Braak *et al.*, 2006). Therefore, we first performed western blots to analyse the

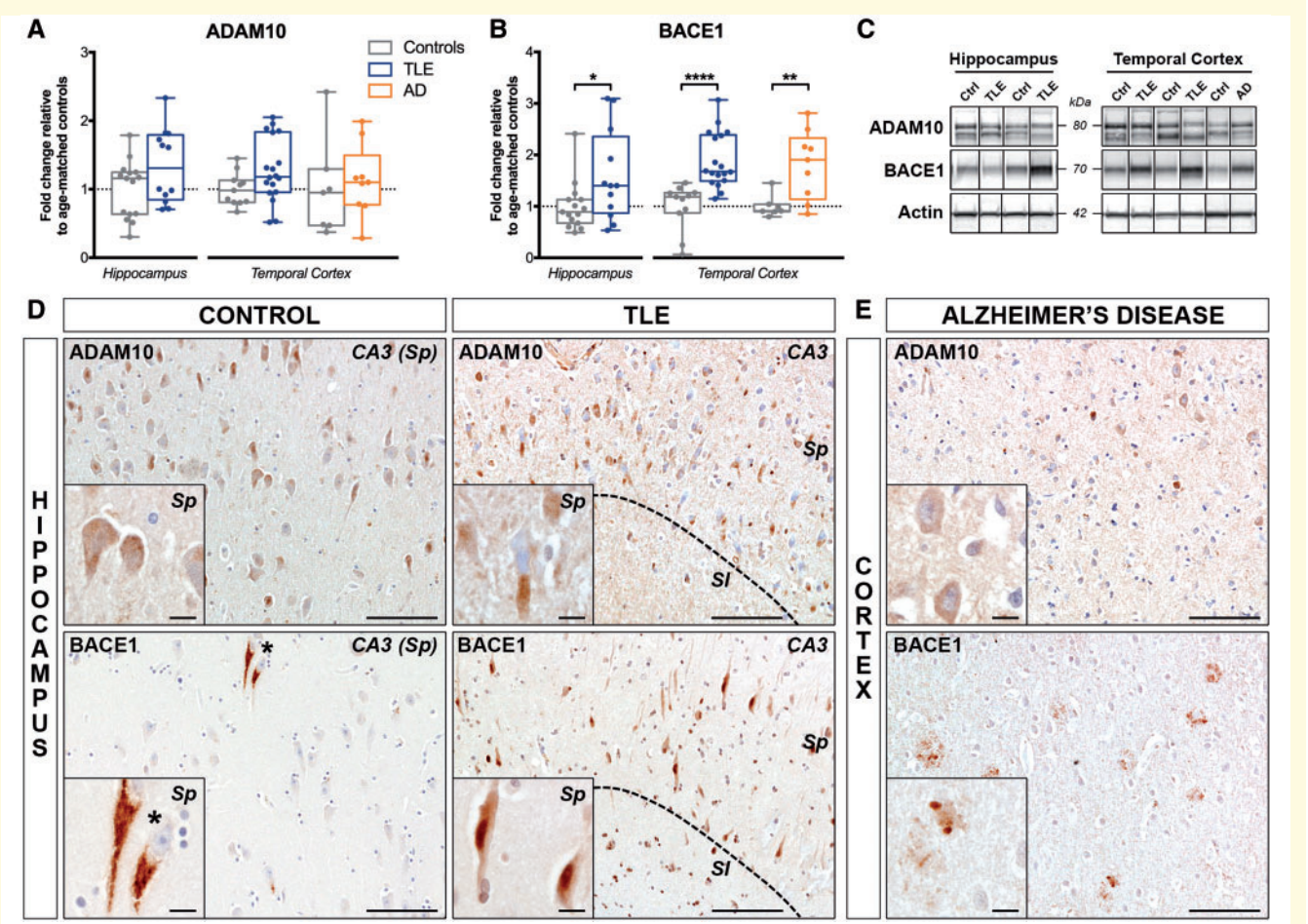

Figure 4 Differential expression of APP processing enzymes ADAM10 and BACE1 in human drug-resistant TLE. (**A** and **B**) Western blot quantification of (**A**) ADAM10 and (**B**) BACE1 in the hippocampus and temporal cortex of TLE, Alzheimer's disease (AD) and control patients. (**C**) Representative western blot images of non-adjacent bands from the same hippocampus or cortex blot. Box-and-whisker plots display the minimum value, the first quartile, the median, the third quartile, and the maximum value. Each group is compared to its respective age-matched control group using two-tailed Student *t*-test (normal distribution) or Mann-Whitney test (skewed distribution). $^{*}P < 0.05$, $^{**}P < 0.01$, $^{****}P < 0.0001$. Detailed statistical data are provided in the Supplementary Table 4. (**D**) Representative images of the hippocampal CA3 pyramidal cell layer from a 55-year-old control subject (Ctrl 15) and a 38-year-old TLE patient with no hippocampal sclerosis (TLE 14) immunohistochemically labelled with ADAM10 (*top row*) showing comparable expression patterns in pyramidal neuron cell bodies of control and TLE cases. Photomicrographs of the hippocampal CA3 pyramidal cell layer from the same control subject (Ctrl 15) and of a 55-year-old TLE patient with hippocampal sclerosis type II (TLE 18) immunohistochemically labelled with BACE1 (*bottom row*) demonstrating increased BACE1 labelling in pyramidal cell bodies and processes in the TLE case relative to control, and occasional BACE1 accumulation in granular-like structures surrounding the nucleus. (**E**) Temporal lobe cortex from a 72-year-old Alzheimer's disease patient immunolabelled with ADAM10 (*top*) and BACE1 (*bottom*) showing faint ADAM10 labelling in neuronal cell bodies and accumulation of BACE1 mostly in fibrillar amyloid plaques. Scale bars = 100 μm in **D** and **E**; *insets* = 10 μm. *Insets* show higher magnification images of the same areas. SI = stratum lucidum; Sp = stratum pyramidale.

expression of total tau, including specific tau isoforms. We used a well-described tau antibody (clone Tau 5), which recognizes all six tau isoforms irrespective of the phosphorylation status (Supplementary Fig. 1D) (Binder *et al.*, 1985), hereafter referred to as tau 5. We found a significant increase in tau 5 expression in TLE hippocampus (297% of controls, $P < 0.01$), but not in the temporal cortex (Fig. 5A). We then analysed the expression of tau isoforms containing either 3 (3R) or 4 (4R) microtubule binding repeats, as in Alzheimer's disease, tau 4R is predominantly expressed in pretangles and tau 3R in neurofibrillary tangles (Hara *et al.*, 2013). Western blot analysis using established isoform-specific antibodies (3R, clone 8E6/C11 and 4R, clone 1E1/A6; Supplementary Fig. 1E and F) (Croft *et al.*, 2018) revealed that tau 3R expression was not altered in TLE relative to controls (Fig. 5B), in contrast to tau 4R levels, which were significantly increased in TLE hippocampus (198% of controls, $P < 0.05$), but not in temporal cortex (Fig. 5C). Neither elevated tau 5 nor tau 4R remained statistically significant after adjustment and correction. As expected, both tau 5 and tau 3R levels were significantly increased in Alzheimer's disease temporal cortex (282% of

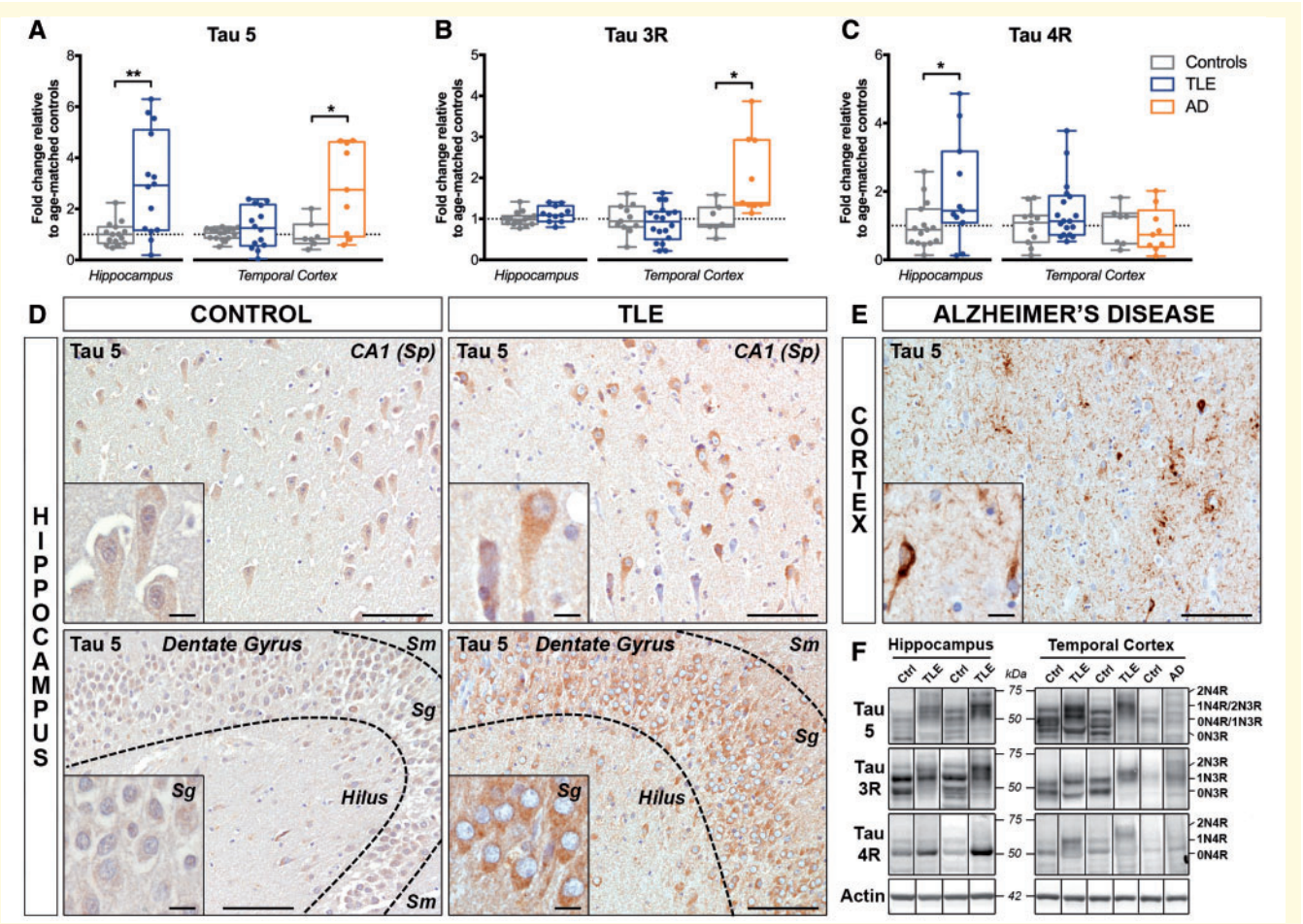

Figure 5 Increased expression of total tau protein in human drug-resistant TLE. (**A**–**C**) Western blot quantification of (**A**) total tau (antibody clone Tau 5), (**B**) tau 3-repeat (Tau 3R), and (**C**) tau 4-repeat (Tau 4R) isoforms in the hippocampus and temporal cortex of TLE, Alzheimer's disease (AD) and control patients. Box-and-whisker plots display the minimum value, the first quartile, the median, the third quartile, and the maximum value. Each group is compared to its respective age-matched control group using two-tailed Student *t*-test (normal distribution) or Mann-Whitney test (skewed distribution). $^{*}P < 0.05$, $^{**}P < 0.01$. Detailed statistical data are provided in Supplementary Table 4. (**D**) Representative images of the hippocampal CA1 pyramidal cell layer (*top row*) from a 55-year-old control subject (Ctrl 15) and a 20-year-old TLE patient with hippocampal sclerosis type I (TLE 6) and of the dentate gyrus (*bottom row*) from a 37-year-old control subject (Ctrl 11) and a 49-year-old TLE patient with hippocampal sclerosis type II (TLE 17), each immunohistochemically labelled with Tau 5 antibody. Images show stronger labelling of neuronal cell bodies and processes in TLE cases compared to controls within both hippocampal regions. (**E**) Temporal lobe cortex from a 65-year-old Alzheimer's disease patient (AD 2) showing typical tau accumulation in neurofibrillary tangles and neuropil threads surrounding amyloid plaques. Scale bars = 100 μm in **D** and **E**; *insets* = 10 μm. *Insets* show higher magnification images of the same areas. (**F**) Representative western blot images for the box-and-whisker plot graphs shown in **A**–**C** representing non-adjacent bands from the same hippocampus or cortex blot. Images show up to four bands, corresponding to tau isoforms 0N3R (55 kDa), 0N4R or 1N3R (64 kDa), 1N4R or 2N3R (69 kDa), and 2N4R (74 kDa). Sg = stratum granulare; Sm = stratum moleculare; Sp = stratum pyramidale.

controls, $P < 0.05$ for tau 5, and 203% of controls, $P < 0.05$ for tau 3R) (Sjogren *et al.*, 2001; Hara *et al.*, 2013), but tau 4R expression was unchanged.

Compared to controls, TLE cases exhibited stronger tau 5 immunoreactivity in CA1–4 regions of the hippocampus (Fig. 5D, top) and the subiculum (not shown), predominantly within the pyramidal neuron cell bodies. Occasionally, prominent nuclear localization of tau 5 was observed, mainly in the hippocampal CA1 (data not shown). Modest staining was seen in the granule cell layer and minimally in the molecular layer of the dentate gyrus (Fig. 5D, bottom). Consistent with the western blot results, TLE cortex did not show these differences relative to controls (data not shown). None of the TLE cases presented tau 5-positive pathological inclusions (neurofibrillary tangles, neuropil threads, neuritic plaques and extracellular 'ghost tangles'), as seen in Alzheimer's disease (Fig. 5E) (Braak *et al.*, 2006).

P-tau was next evaluated using two different antibodies (Supplementary Fig. 1G and H) recognizing well-established serine and threonine epitopes: p-tau AT8 (Ser202/Thr205), found in Alzheimer's disease neurofibrillary tangles and ghost tangles, and p-tau AT180 (Thr231), associated mostly with pretangles (Augustinack *et al.*, 2002). Western blot analysis demonstrated that p-tau AT8 expression was significantly increased in both TLE hippocampus (230% of controls, $P < 0.001$) and temporal cortex (261% of controls, $P < 0.0001$) (Fig. 6A), consistent with the previously observed increased AT8 immunoreactivity in TLE patients (Thom *et al.*, 2011; Tai *et al.*, 2016). Similarly, p-tau AT180 showed a significant increase in TLE hippocampus (292% of controls, $P < 0.0001$) and temporal cortex (180% of controls, $P < 0.001$) (Fig. 6B). Both p-tau AT8 and AT180 results remained significant after adjustment for co-variables and correction for the number of markers. When comparing p-tau to tau 5 ratios, only p-tau AT180/tau 5 was significantly increased in TLE hippocampus (244% of controls, $P < 0.01$) and cortex (454% of controls, $P < 0.05$, Supplementary Fig. 3). As anticipated, the Alzheimer's disease cases showed a more robust increase in both p-tau AT8 (18 700% of controls, $P < 0.001$) and p-tau AT180 (1859% of controls, $P < 0.0001$) (Fig. 6A and B), and significantly higher p-tau AT8/tau 5 (5524% of controls, $P < 0.0001$) and p-tau AT180/tau 5 (860% of controls, $P < 0.01$) ratios (Supplementary Fig. 4).

As p-tau AT8 immunostaining has already been described in human chronic epilepsy (Thom *et al.*, 2011; Iyer *et al.*, 2014; Puvenna *et al.*, 2016; Tai *et al.*, 2016), we focused on the early pretangle marker p-tau AT180. TLE cases demonstrated stronger somatic p-tau AT180 immunoreactivity in all hippocampal subfields, including CA1–4 (Fig. 6D, top) and dentate gyrus (Fig. 6D, bottom), when compared to controls. The reactivity in epilepsy patient samples was diffuse across layers, but most obvious in large pyramidal neurons and granule cells (Supplementary Fig. 2B). Most AT180-labelled neurons presented diffuse cytoplasmic staining, with no evident intracellular inclusions, resembling the typical Alzheimer's disease pre-neurofibrillary tangles (Augustinack *et al.*, 2002). Co-immunofluorescence of AT180 with GFAP demonstrated no expression in astrocytes (Fig. 6E, top), while co-labelling with the neuronal marker MAP2 confirmed increased p-tau AT180 labelling in the neuronal cell bodies and processes (Fig. 6E, bottom). A similar pattern was observed in the temporal cortex (Fig. 6F). As expected, p-tau AT180 immunoreactivity was much stronger in Alzheimer's disease cases, where it mostly stained pathological inclusions (Fig. 6G and Supplementary Fig. 2).

Selective dysregulation of stress-response pathways in human temporal lobe epilepsy

To determine potential mechanisms for the observed amyloid and tau-related neurodegenerative changes in human TLE, we next assessed the activation status of several known cell-stress pathways involved in Alzheimer's disease pathogenesis by promoting pathological forms of amyloid and tau through transcriptional, translational and post-translational mechanisms (Aplin *et al.*, 1996; Iijima *et al.*, 2000; Standen *et al.*, 2001; O'Connor *et al.*, 2008; Tamagno *et al.*, 2012; Martin *et al.*, 2013; Wang *et al.*, 2013) (Fig. 1).

The activation status of JNK, p70S6K, GSK-3β, PERK and eIF2α kinases was assessed by western blot quantification of known activating phosphorylation sites (p): Thr183/Tyr185 for JNK (Ip and Davis, 1998), Thr389 for p70S6K (Hornberger *et al.*, 2007), Tyr216 for GSK-3β (Bhat *et al.*, 2000), Ser713 for PERK (Devi and Ohno, 2014), and Ser51 for eIF2α (O'Connor *et al.*, 2008). CDK5 activity was determined indirectly by quantifying the relative abundance of its activator p35 protein versus its cleavage product p25 (Patrick *et al.*, 1999), while PP2A activation was assessed by quantification of its inhibitory phosphorylation at Tyr307 (Chen *et al.*, 1992).

Phospho-JNK/JNK and p-p70S6K/p70S6K ratios were both significantly increased in TLE hippocampus (1896% of controls, $P < 0.0001$ and 429%, $P < 0.0001$, respectively) and temporal cortex (839% of controls, $P < 0.0001$ and 347% of controls, $P < 0.001$, respectively) (Fig. 7A and B). In contrast, pGSK-3β/GSK-3β and p25/p35 ratios were significantly decreased in TLE hippocampus (30% of controls, $P < 0.001$ and 36% of controls, $P < 0.01$, respectively) and temporal cortex (39% of controls, $P < 0.001$ and 44% of controls, $P < 0.01$, respectively) (Fig. 7C and D). Phospho-PERK/PERK and peIF2α/eIF2α ratios were significantly increased in both TLE hippocampus (389% of controls, $P < 0.001$ and 163% of controls, $P < 0.05$, respectively) and temporal cortex (1020% of controls, $P < 0.0001$ and 157% of controls, $P < 0.01$) (Fig. 7E and F). Phospho-JNK/JNK, p-p70S6K/p70S6K and pGSK-3β/GSK-3β ratios remained significant in both brain regions after adjustment and correction, while pPERK/PERK ratios remained significant only in the hippocampus and peIF2α/eIF2α only in the temporal cortex (Supplementary Tables 4 and 5). The Alzheimer's disease temporal cortex

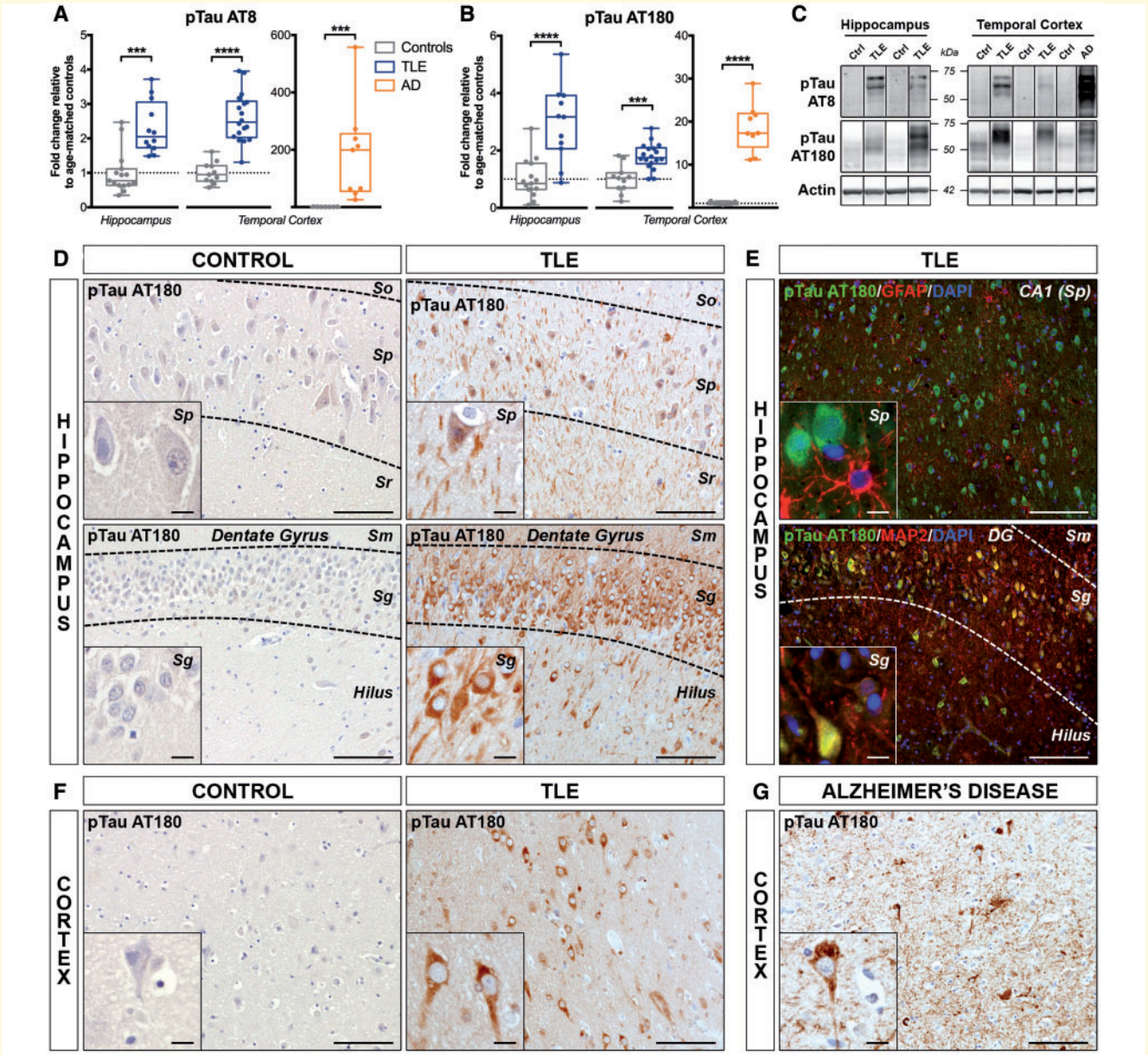

Figure 6 Increased phosphorylation of tau in human drug-resistant TLE. (**A** and **B**) Western blot quantification of (**A**) phospho-tau [Ser202/Thr205] (antibody clone AT8) and (**B**) phospho-tau [Thr231] (antibody clone AT180) in the hippocampus and temporal cortex of TLE, Alzheimer's disease (AD) and control patients. Box-and-whisker plots display the minimum value, the first quartile, the median, the third quartile, and the maximum value. Each group is compared to its respective age-matched control group using two-tailed Student *t*-test (normal distribution) or Mann-Whitney test (skewed distribution). $^{***}P < 0.001$, $^{****}P < 0.0001$. Detailed statistical data are provided in Supplementary Table 4. (**C**) Representative western blot images of individual proteins depicting non-adjacent bands originating from the same blot. (**D**) Photomicrographs of hippocampal CA1 pyramidal cell layer (*top row*) and of granular layer of the dentate gyrus (*bottom row*) from a 37-year-old control subject (Ctrl 11) and a 49-year-old TLE patient with hippocampal sclerosis type II (TLE 17) immunohistochemically labelled with p-tau AT180. Images show greater accumulation of p-tau AT180 in neuronal cell bodies and processes within the hippocampal CA1 pyramidal cell layer and DG granular layer in the TLE case compared to control. (**E**, *top*) Hippocampal CA1 pyramidal cell layer of a 49-year-old TLE patient with hippocampal sclerosis type II (TLE 17), co-immunolabelled with p-tau AT180 (green), astrocytic marker GFAP (red), and nuclear stain DAPI (blue) showing no colocalization of p-tau AT180 with GFAP. (**E**, *bottom*) Representative section of the dentate gyrus (DG) region from a 12-year-old TLE patient with hippocampal sclerosis type II (TLE 3), co-immunolabelled with p-tau AT180 (green), MAP2 (red) and nuclear stain DAPI (blue) demonstrating co-localization of p-tau AT180 with neuronal cell bodies and processes. A similar p-tau AT180 expression pattern is evident with both diaminobenzidine (**D**) and immunofluorescence (**E**) labelling. (**F**) Representative temporal cortex sections from a 20-year-old control subject (Ctrl 6) and a 49-year-old TLE patient (TLE 17) immunohistochemically labelled with p-tau AT180 show more robust labelling of neuronal cell bodies and processes in the TLE case compared to the control subject. (**G**) Temporal lobe cortex images from a 65-year-old Alzheimer's disease patient (AD 2) showing accumulation of p-tau AT180 in neurofibrillary tangles and neuropil threads surrounding amyloid plaques. Scale bars = 100 μm in **D**–**G**; *insets* = 10 μm. *Insets* show higher magnification images of the same areas. Sg = stratum granulare; Sm = stratum moleculare; So = stratum oriens; Sp = stratum pyramidale; Sr = stratum radiatum.

showed both increased pJNK/JNK (145% of controls, $P < 0.05$) and peIF2α/eIF2α (151% of controls, $P < 0.05$) ratios.

Phospho-PP2A/PP2A ratios showed no significant changes in TLE brain samples, but total PP2A was significantly decreased in TLE temporal cortex (71% of controls, $P < 0.001$), and this remained significant after adjustment for covariates and correction for multiple comparisons (Supplementary Fig. 4 and Supplementary Tables 4 and 5). Phospho-PP2A/PP2A and PP2A showed no significant changes in Alzheimer's disease brain samples.

Correlation analysis between biochemical variables in temporal lobe epilepsy

Correlation analysis between individual biochemical markers adjusted for age at surgery, gender, and disease duration revealed a positive correlation between BACE1 and full-length APP in both TLE hippocampus ($P < 0.05$, r = 0.77) and temporal cortex ($P < 0.05$, r = 0.55) (Fig. 8A). In TLE hippocampus, amyloid-β_{42}-degrading enzyme neprilysin expression was positively correlated with amyloid-β_{42} oligomers ($P < 0.05$, r = 0.89) and total PP2A expression was negatively correlated with p-tau AT8 ($P < 0.05$, r = –0.72) (Fig. 8A). In TLE temporal cortex, activated JNK was positively correlated with BACE1 ($P < 0.001$, r = 0.81), activated PERK levels were positively correlated with both p-tau AT8 ($P < 0.01$, r = 0.65) and AT180 levels ($P < 0.05$, r = 0.6), while amyloid-β_{42} was positively correlated with tau 4R ($P < 0.05$, r = 0.52) (Fig. 8A). In addition, we observed a correlation between the two p-tau species, which was negative in the hippocampus ($P < 0.05$, r = –0.72), but positive in the cortex ($P < 0.05$, r = 0.61) (Fig. 8A). We also found a few unexpected negative correlations: between amyloid-β_{42} and tau 5 ($P < 0.05$, r = –0.75) and between amyloid-β*56 and activated JNK ($P < 0.01$, r = –0.82) in the hippocampus, and between APP and p-tau AT8 ($P < 0.05$, r = –0.52), between amyloid-β*56 and the two p-tau species ($P < 0.05$, r = –0.57 and –0.53 with AT8 and AT180, respectively), as well as between amyloid-β_{42} and activated p70S6K ($P < 0.05$, r = –0.56) in the cortex (Fig. 8A).

Correlation analysis with hippocampal pathology, epilepsy characteristics and cognitive decline

Hippocampal APP, pAPP, tau 5, p-tau AT180 and pGSK-3β/GSK-3β levels were specifically associated with hippocampal sclerosis, while p70S6K activation was associated with non-sclerotic hippocampal pathology. Amyloid-β*56, p-tau AT180 and pJNK/JNK levels were independent of hippocampal pathology. Hippocampal pathology had no impact on cortical biochemical markers analysed, except for p-p70S6K/p70S6K and peIF2α/eIF2α ratios, which were individually associated with either hippocampal sclerosis or with non-sclerotic pathology, respectively (Supplementary Table 5). We also examined potential associations between biochemical markers and seizure focus location. Hippocampal pAPP, p-tau AT180 and pGSK-3β/GSK-3β ratios were associated with a hippocampal seizure onset, while amyloid-β_{42}, neprilysin and pPERK/PERK ratios

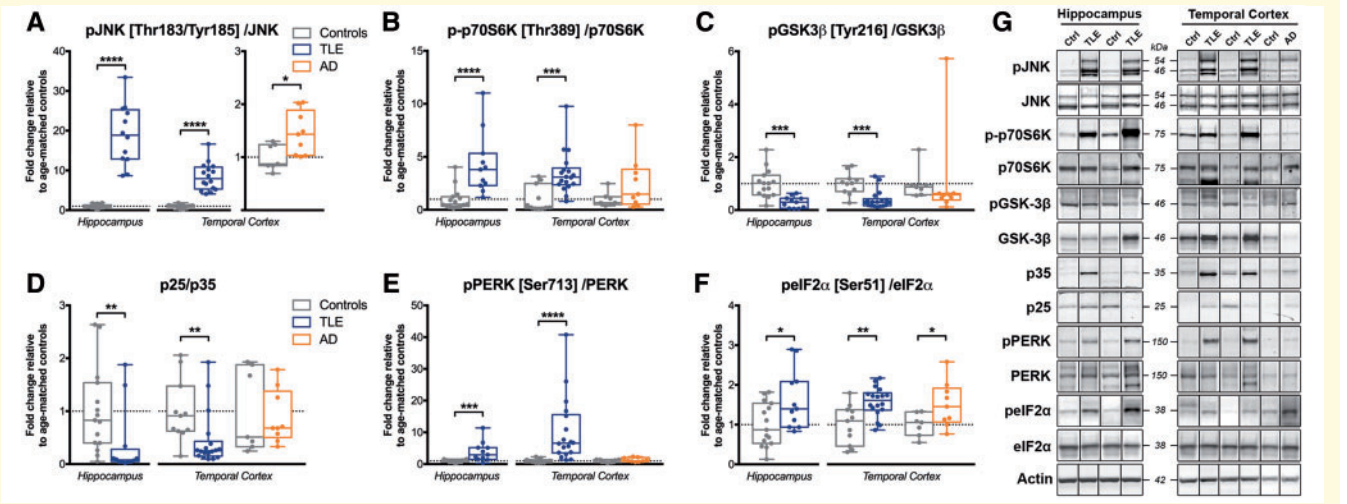

Figure 7 Dysregulation of JNK, p70S6K, GSK-3β, p25/p35 and PERK/eIF2α signalling in human drug-resistant TLE. (**A–F**) Western blot quantification of (**A**) phospho-JNK [Thr183/Tyr185]/JNK, (**B**) phospho-p70S6K [Thr389]/p70S6K, (**C**) phospho-GSK-3β [Tyr216]/GSK-3β, (**D**) p25/p35, (**E**) phospho-PERK [Ser713]/PERK, and (**F**) phospho-eIF2α [Ser51]/eIF2α ratios in the hippocampus and temporal cortex of TLE, Alzheimer's disease (AD) and control (Ctrl) patients. Box-and-whisker plots display the minimum value, the first quartile, the median, the third quartile, and the maximum value. Each group is compared to its respective age-matched control group using two-tailed Student *t* test (normal distribution) or Mann-Whitney test (skewed distribution). $^{*}P < 0.05$, $^{**}P < 0.01$, $^{***}P < 0.001$, $^{****}P < 0.0001$. Detailed statistical data are provided in the Supplementary Table 4. (**G**) Representative western blot images of individual proteins depicting non-adjacent bands originating from the same blot.

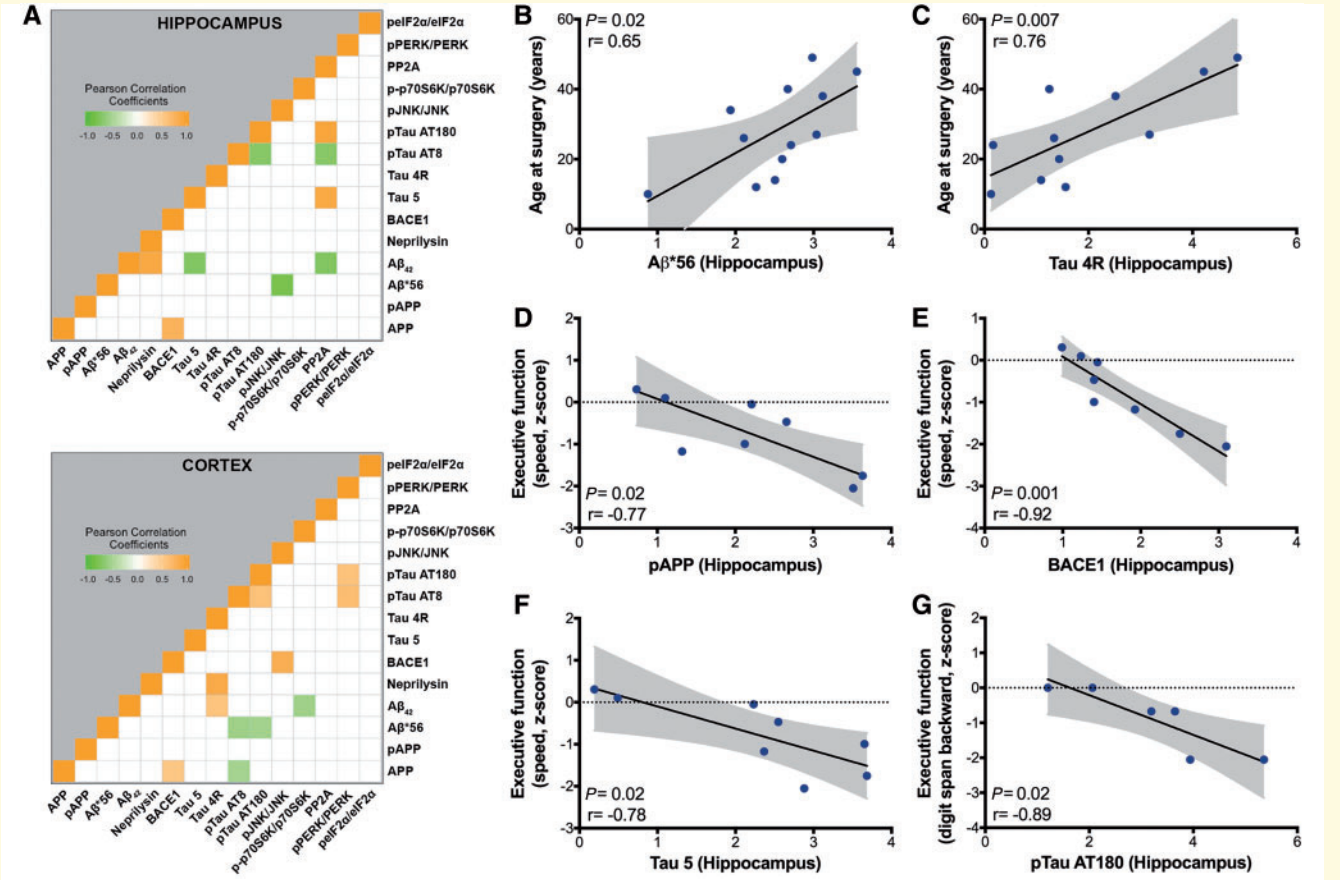

Figure 8 Correlations between Alzheimer's disease-like pathology markers, age at surgery and cognitive scores from pre-operative assessment in human drug-resistant TLE. (**A**) Heat map showing the Pearson correlation matrix between the biological markers analysed by western blot in the hippocampus (*top*) and cortex (*bottom*) from TLE cases adjusted for gender, age at surgery and disease duration (n = 11–18). (**B** and **C**) Pearson correlations in TLE hippocampus show positive relationships between age at surgery and unadjusted hippocampal **(B)** amyloid-β*56 (n = 12) and (**C**) tau 4-repeat isoforms (Tau 4R, n = 11) expression. (**D-F**) Pearson correlations in adult TLE hippocampus showing negative relationships between executive function assessed by the processing speed efficiency test, expressed as z-scores, and unadjusted hippocampal (**D**) pAPP (n = 8), (**E**) BACE1 (n = 8), and (**F**) total tau (Tau 5, n = 8) protein expression. (**G**) Pearson correlation in adult TLE hippocampus showing negative relationships between executive function assessed by the digit span backward test, expressed as z-scores, and unadjusted hippocampal p-tau AT180 (n = 6) expression. Grey area indicates 95% confidence interval for the two means for each graph.

were associated with an extra-hippocampal seizure focus. Amyloid-β*56, p-tau AT8 and pJNK/JNK ratios were independent of seizure focus location. In temporal cortex, most of the markers were independent of seizure focus location, except for p25/p35, p-p70S6K/p70S6K and peIF2α/eIF2α ratios, which were found to be associated with a hippocampal seizure onset (Supplementary Table 5).

Age at surgery correlated strongly with hippocampal amyloid-β*56 ($P < 0.05$, r = 0.65) and tau 4R levels ($P < 0.01$, r = 0.76) (Fig. 8B and C), as reported in Alzheimer's disease patients (Braak *et al.*, 2013), while age at seizure onset and epilepsy duration did not correlate with any of the biochemical measures. Correlations with pre-operative cognitive z-scores demonstrated negative correlations between executive function, assessed by the processing speed efficiency, and hippocampal pAPP ($P < 0.05$, r = –0.77), BACE1 ($P = 0.001$, r = –0.92) and tau 5 ($P < 0.05$, r = –0.78) (Fig. 8D–F). P-tau AT180 expression was negatively correlated with another test measuring impaired executive function (digit span backward test, $P < 0.05$, r = –0.89) (Fig. 8G).

Discussion

Interictal cognitive impairment is a major issue in TLE and can be progressive over time (Hermann *et al.*, 2006; Berg *et al.*, 2012). Chronic epilepsy has been associated with accelerated brain ageing (Dabbs *et al.*, 2012; Joutsa *et al.*, 2017; Pardoe *et al.*, 2017), suggesting that degenerative mechanisms may be at least in part responsible for these changes, especially in the hippocampus, a key area involved in cognitive function and significantly engaged in TLE.

Both amyloid expression and tau hyperphosphorylation have been previously reported to be increased in drug-resistant TLE tissue via immunohistochemistry (Mackenzie and Miller, 1994; Sheng *et al.*, 1994; Thom *et al.*, 2011; Sima *et al.*, 2014; Tai *et al.*, 2016). The present study builds upon these

observations to examine multiple steps in the amyloid and tau pathogenic cascades to identify candidate mechanisms that may underlie an interaction between hyperexcitability, Alzheimer-like neuropathology and cognition. Our overall hypothesis was that network hyperexcitability in TLE activates signalling pathways known to upregulate pathological forms of amyloid and tau, which, in turn, could cause neuronal dysfunction and cognitive impairment (Fig. 1).

Our novel results show that human drug-resistant TLE tissue exhibits several molecular changes resembling those seen in patients with Alzheimer's disease, some of which were strongly correlated with impaired preoperative executive function. In addition, we found strong correlations between two degeneration markers and age at surgery, implying that ageing might be a risk factor for the development of Alzheimer-like pathology in TLE. We also found alterations in a wide range of molecular pathways known to be upstream and downstream of amyloid and tau production, and because of the large number of parameters included, we were able to test novel relationships between these pathway components.

There is compelling evidence that uncontrolled seizures have negative effects on cognition over time (Taylor *et al.*, 2010; Berg *et al.*, 2012). Epilepsy more broadly may contribute to cognitive deterioration, as in addition to seizures, interictal spikes located either inside or outside of the seizure onset zone are associated with altered learning and memory (Kleen *et al.*, 2013; Gelinas *et al.*, 2016; Ung *et al.*, 2017). However, other studies show that in nearly half of patients, cognitive impairments are present at the time of first diagnosis (Taylor *et al.*, 2010; Witt and Helmstaedter, 2012), raising the possibility of common pathophysiological mechanisms.

Another disorder in which there is cognitive dysfunction involving the temporal lobe is Alzheimer's disease, although cognitive symptoms in Alzheimer's disease are distinguishable from those seen in TLE (Tellechea *et al.*, 2018). Hippocampal hyperexcitability and epileptiform discharges (Vossel *et al.*, 2016; Lam *et al.*, 2017) are common occurrences in patients with Alzheimer's disease, which can lead to accelerated cognitive decline (Yan *et al.*, 2012). Alzheimer's disease patients, in particular those with the genetic early-onset familial disease, have a 10-fold increased risk of developing seizures (Vossel *et al.*, 2017). Together, these data highlight a potential bidirectional relationship between hyperexcitability, Alzheimer's disease pathology and cognition.

APP and its amyloidogenic processing in human temporal lobe epilepsy

Here we show that APP expression is elevated in hippocampal tissue from drug-resistant TLE. The implications of this finding are potentially broad. Full length APP is normally expressed at both pre- and postsynaptic sites, functioning as an adhesion molecule to stabilize synapses and increase synaptic transmission (Hoe *et al.*, 2009; Lee *et al.*, 2010). Hence, APP upregulation in TLE hippocampus seen here may contribute to seizure-induced synaptogenesis, axonal sprouting and neurite outgrowth (Westmark, 2013) and promote network hyperexcitability. Indeed, mice overexpressing APP (Moechars *et al.*, 1999; Mucke *et al.*, 2000; Lalonde *et al.*, 2005; Palop *et al.*, 2007; Westmark and Malter, 2007; Roberson *et al.*, 2011; Ziyatdinova *et al.*, 2011; Chin and Scharfman, 2013; Born *et al.*, 2014; Born, 2015; Pasciuto *et al.*, 2015) show increased excitability and epileptiform discharges, which can be rescued by restoring normal APP levels.

Further, our data show that in drug-resistant TLE, elevated APP is preferentially processed through the amyloidogenic pathway, similar to Alzheimer's disease, as demonstrated by increased pAPP, amyloid-β*56 and amyloid-β_{42} expression, and the strong positive correlation between APP and BACE1 levels, but not ADAM10. As NMDA receptor activity favours APP trafficking and β-cleavage by BACE1 over α-cleavage by ADAM10 (Hoe *et al.*, 2009), it is possible that chronic seizures may be responsible for such changes (Yan *et al.*, 2012; Jang *et al.*, 2016; Kodam *et al.*, 2019). In addition, neprilysin expression was not downregulated in TLE tissue and was correlated with amyloid-β_{42}, suggesting a strong compensatory response, in stark contrast with Alzheimer's disease where this pathway is highly downregulated (Miners *et al.*, 2006).

The amyloidogenic APP cleavage product amyloid-β*56 accumulates before amyloid-β_{42} dimers and is associated with memory impairment (Lesne *et al.*, 2006). Furthermore, amyloid-β*56 interacts with NMDA receptors and promotes tau hyperphosphorylation (Amar *et al.*, 2017). Amyloid-β_{42} accumulation, in addition to being linked with cognitive dysfunction, can trigger abnormal network synchronization (Noebels, 2011) and ultimately epileptic activity (Westmark *et al.*, 2008; Palop and Mucke, 2009). Neither amyloid-β*56 nor amyloid-β_{42} were associated with decreased cognitive performance in our adult TLE cases, consistent with a recent imaging study showing no correlation between increased amyloid accumulation and reduced cognitive performance in adults with chronic epilepsy (Joutsa *et al.*, 2017). In contrast, pAPP and BACE1 were both negatively correlated with executive function, which is intriguing and deserves further investigation. BACE1 cleaves many other proteins and it is possible that biological functions independent of APP processing may also lead to cognitive impairment in TLE (Yan, 2017). Future genome-wide association studies in TLE patients, as performed in Alzheimer's disease (Kunkle *et al.*, 2019), are warranted and may uncover novel genetic variants affecting APP and amyloid-β processing and cognitive function.

Tau 5, hyperphosphorylated tau and temporal lobe epileptogenesis

While this study provides evidence for enhanced amyloidogenic APP processing in TLE, we also demonstrate complex

changes involving the microtubule-associated protein tau. Tau 5 is predominantly expressed in axons and participates in axonal transport and outgrowth; however, tau 5 overexpression in dendrites and spines can impair synaptic function causing memory deficits in mice (Zhao *et al.*, 2016). Tau 5 protein has been associated with cognitive decline in several neurodegenerative diseases, including Alzheimer's disease, which is consistent with our study demonstrating a negative correlation between hippocampal tau 5 expression and executive function in TLE. In rodent Alzheimer's disease and epilepsy models, tau 5 was also shown to promote neuronal excitability (Roberson *et al.*, 2011; DeVos *et al.*, 2013; Holth *et al.*, 2013), while in epilepsy patients, elevated tau 5 levels in the CSF have been correlated with seizure type and duration (Tumani *et al.*, 2015). Altered tau 4R/tau 3R isoform ratios, as we found in TLE hippocampus can trigger neurodegeneration, and there is evidence that tau 4R has a great impact on tau pathology, neuronal hyperexcitability and cognitive dysfunction in animal models (Schoch *et al.*, 2016; Espindola *et al.*, 2018).

Pathological phosphorylation of tau leads to its dissociation from the microtubules and its aggregation into neurofibrillary tangles, the hallmark of several neurodegenerative cognitive disorders, including Alzheimer's disease (Iqbal *et al.*, 2005). Several studies have demonstrated that seizures can promote abnormal tau phosphorylation (Crespo-Biel *et al.*, 2007; Liang *et al.*, 2009; Tian *et al.*, 2010; Jones *et al.*, 2012; Liu *et al.*, 2016). Most importantly, pharmacological interventions reducing p-tau levels have been shown to have both anti-seizure and anti-epileptogenic effects in animal models (Jones *et al.*, 2012; Gheyara *et al.*, 2014; Li *et al.*, 2014, Liu *et al.*, 2016).

Targeting cell-stress pathways as novel therapeutic strategies for temporal lobe epilepsy with cognitive dysfunction

Finally, our study raises the possibility of novel specific molecular mechanisms underlying Alzheimer-like neurodegenerative processes in drug-resistant TLE that may be targeted for disease modification. Of the main stress kinases involved in APP and/or tau 5 phosphorylation in Alzheimer's disease (Aplin *et al.*, 1996; Iijima *et al.*, 2000; Standen *et al.*, 2001; Wang *et al.*, 2013), only JNK and mTOR/p70S6K appeared to be activated in TLE in agreement with previous reports (Liu *et al.*, 2011; Talos *et al.*, 2018). JNK activation was positively correlated with BACE1 protein expression in TLE cortex, consistent with its role in *BACE1* transcriptional upregulation (Tamagno *et al.*, 2012). However, its phosphorylation level did not correlate with pAPP or p-tau expression, suggesting the involvement of other activity-dependent kinases, such as ERK or cyclic AMP-dependent protein kinase (Rakhade *et al.*, 2008; Talos *et al.*, 2018) in these events. Nevertheless, JNK inhibition in TLE may be a therapeutic strategy to improve both cognition and seizure outcomes, given its effects on BACE1, and its proven antiepileptic and neuroprotective properties in rodent epilepsy models (Chen *et al.*, 2010; Spigolon *et al.*, 2010; Tai *et al.*, 2017). Relevant to our finding of increased mTOR/p70S6K signalling, multiple animal models of TLE have shown that mTOR inhibitor rapamycin prevents epilepsy and the cellular alterations involved in epileptogenesis, including neuronal death and mossy fibre sprouting (Buckmaster *et al.*, 2009; Zeng *et al.*, 2009; Huang *et al.*, 2010; Goto *et al.*, 2011; van Vliet *et al.*, 2012). The present study suggests other mechanisms upstream and downstream of mTOR are involved, making this target exceptionally promising.

Besides JNK and mTOR/p70S6K, we found that the PERK/eIF2α pathway is also activated in drug-resistant TLE, as observed in neurodegenerative cognitive diseases (O'Connor *et al.*, 2008; Hoozemans *et al.*, 2012), extending our understanding of the pathways leading to increased endoplasmic reticulum stress in sclerotic hippocampus from TLE patients (Yamamoto *et al.*, 2006; Liu *et al.*, 2011). In response to endoplasmic reticulum stress, PERK/eIF2α activation induces a chronic inhibition of protein translation that can lead to neuronal degeneration and loss (Moreno *et al.*, 2012). In addition, the activated PERK/eIF2α pathway also paradoxically favours the translation of particular mRNAs, including *BACE1* (O'Connor *et al.*, 2008). In Alzheimer's disease mouse models, inhibition of PERK/eIF2α activity decreases the translation of *BACE1* mRNA and improves synaptic plasticity and memory decline, and therefore a similar molecular strategy could be used for drug-resistant TLE treatment. A more direct BACE1 inhibition, with the same inhibitory agents currently tested in Alzheimer's disease (Cummings *et al.*, 2018), may thus be of potential benefit in TLE patients with cognitive deficits.

We acknowledge that our study has limitations, as the patients studied here represent a particular subgroup of TLE cases with severe, drug-resistant epilepsy, and by the exclusive examination of the hippocampus and temporal lobe region, we have likely not captured the full spectrum of degenerative changes present in the TLE brain. Inherent for most studies conducted in human specimens, we were also limited by the relative small number of cases available to us, especially in the paediatric age range, which precluded us to perform further subgroup analyses.

Conclusion

The present data supports an interaction between hyperexcitability in epilepsy and amyloid and tau-related neurodegeneration that may underlie cognitive impairment in drug-resistant TLE. The detailed and novel observations here suggest that therapeutic interventions targeting these pathways may be beneficial for treating cognitive decline in TLE. This study also suggests that particular proteins could be useful

biomarkers in accurately identify drug-resistant TLE patients at risk of developing cognitive disabilities.

Acknowledgements

We are grateful to Dr Gregory Heuer (Department of Neurosurgery, Children's Hospital of Philadelphia) for providing us two paediatric tissue samples for this study. We also thank Dr Dara Fisher (Penn Neuroscience Center, Perelman Center for Advanced Medicine) for assistance with the neuropsychological dataset and Theresa Schuck (Center for Neurodegenerative Disease Research at the University of Pennsylvania) for her help with human tissue retrieval.

Funding

This work was supported by grants from the National Institutes of Health/National Institute of Neurological Disorders and Stroke (NIH/NINDS): R01NS101156 (D.M.T.), R21NS105437 (F.E.J.), R01NS080565 (F.E.J.), K23NS088341 (D.J.I.) and K23NS092973 (K.A.D.); the University Research Foundation (D.M.T.); the Brightfocus Foundation A2016244S (D.J.I.); the Penn Institute on Aging (D.J.I.). This research was supported in part by the Repository Core for Neurological Disorders, Department of Neurology, Boston Children's Hospital, and the Intellectual And Developmental Disabilities Research Center IDDRC supported by the NIH P30HD018655. We thank the Center for Neurodegenerative Disease Research (CNDR) at the University of Pennsylvania for providing us with post-mortem Alzheimer's disease and control tissue for the study. The CNDR has been supported by the NIH/National Institute on Aging AG010124. Additional control human tissue was obtained from University of Maryland Brain and Tissue Bank, which is a Brain and Tissue Repository of the NIH NeuroBioBank.

Competing interests

D.M.T. and F.E.J. and K.A.D. have received investigator-initiated research grants unrelated to this work from Eisai Co., Ltd. and have served at scientific advisory board meetings for Eisai Co., Ltd. K.A.D. has served as an advisory board member for H. Lundbeck A/S and as consultant for UCB. E.D.M. is a scientific advisory council member for CURE (Citizens United for Research in Epilepsy) and has served as a consultant for Stoke Therapeutics, and as scientific advisory board member for LGS foundation and Eisai Co., Ltd. All other authors report no competing interests.

Supplementary material

Supplementary material is available at *Brain* online.

References

Amar F, Sherman MA, Rush T, Larson M, Boyle G, Chang L, et al. The amyloid-beta oligomer Abeta*56 induces specific alterations in neuronal signaling that lead to tau phosphorylation and aggregation. Sci Signal 2017; 10: eaal2021.

Aplin AE, Gibb GM, Jacobsen JS, Gallo JM, Anderton BH. In vitro phosphorylation of the cytoplasmic domain of the amyloid precursor protein by glycogen synthase kinase-3beta. J Neurochem 1996; 67: 699–707.

Appenzeller-Herzog C, Hall MN. Bidirectional crosstalk between endoplasmic reticulum stress and mTOR signaling. Trends Cell Biol 2012; 22: 274–82.

Asadi-Pooya AA, Stewart GR, Abrams DJ, Sharan A. Prevalence and incidence of drug-resistant mesial temporal lobe epilepsy in the United States. World Neurosurg 2017; 99: 662–66.

Augustinack JC, Schneider A, Mandelkow EM, Hyman BT. Specific tau phosphorylation sites correlate with severity of neuronal cytopathology in Alzheimer's disease. Acta Neuropathol 2002; 103: 26–35.

Berg AT, Zelko FA, Levy SR, Testa FM. Age at onset of epilepsy, pharmacoresistance, and cognitive outcomes: a prospective cohort study. Neurology 2012; 79: 1384–91.

Bhat RV, Shanley J, Correll MP, Fieles WE, Keith RA, Scott CW, et al. Regulation and localization of tyrosine216 phosphorylation of glycogen synthase kinase-3beta in cellular and animal models of neuronal degeneration. Proc Natl Acad Sci U S A 2000; 97: 11074–9.

Binder LI, Frankfurter A, Rebhun LI. The distribution of tau in the mammalian central nervous system. J Cell Biol 1985; 101: 1371–8.

Blumcke I, Spreafico R, Haaker G, Coras R, Kobow K, Bien CG, et al. Histopathological findings in brain tissue obtained during epilepsy surgery. N Engl J Med 2017; 377: 1648–56.

Blumcke I, Thom M, Aronica E, Armstrong DD, Bartolomei F, Bernasconi A, et al. International consensus classification of hippocampal sclerosis in temporal lobe epilepsy: a Task Force report from the ILAE Commission on Diagnostic Methods. Epilepsia 2013; 54: 1315–29.

Blumcke I, Thom M, Aronica E, Armstrong DD, Vinters HV, Palmini A, et al. The clinicopathologic spectrum of focal cortical dysplasias: a consensus classification proposed by an ad hoc Task Force of the ILAE Diagnostic Methods Commission. Epilepsia 2011; 52: 158–74.

Born HA. Seizures in Alzheimer's disease. Neuroscience 2015; 286: 251–63.

Born HA, Kim JY, Savjani RR, Das P, Dabaghian YA, Guo Q, et al. Genetic suppression of transgenic APP rescues Hypersynchronous network activity in a mouse model of Alzeimer's disease. J Neurosci 2014; 34: 3826–40.

Braak H, Alafuzoff I, Arzberger T, Kretzschmar H, Del Tredici K. Staging of Alzheimer disease-associated neurofibrillary pathology using paraffin sections and immunocytochemistry. Acta Neuropathol 2006; 112: 389–404.

Braak H, Zetterberg H, Del Tredici K, Blennow K. Intraneuronal tau aggregation precedes diffuse plaque deposition, but amyloid-beta changes occur before increases of tau in cerebrospinal fluid. Acta Neuropathol 2013; 126: 631–41.

Buckmaster PS, Ingram EA, Wen X. Inhibition of the mammalian target of rapamycin signaling pathway suppresses dentate granule cell axon sprouting in a rodent model of temporal lobe epilepsy. J Neurosci 2009; 29: 8259–69.

Caccamo A, Branca C, Talboom JS, Shaw DM, Turner D, Ma L, et al. Reducing ribosomal protein S6 kinase 1 expression improves spatial memory and synaptic plasticity in a mouse model of Alzheimer's disease. J Neurosci 2015; 35: 14042–56.

Caccamo A, Magri A, Medina DX, Wisely EV, Lopez-Aranda MF, Silva AJ, et al. mTOR regulates tau phosphorylation and

degradation: implications for Alzheimer's disease and other tauopathies. Aging Cell 2013; 12: 370–80.
Caccamo A, Majumder S, Richardson A, Strong R, Oddo S. Molecular interplay between mammalian target of rapamycin (mTOR), amyloid-beta, and Tau: effects on cognitive impairments. J Biol Chem 2010; 285: 13107–20.
Carnevalli LS, Pereira CM, Jaqueta CB, Alves VS, Paiva VN, Vattem KM, et al. Phosphorylation of the alpha subunit of translation initiation factor-2 by PKR mediates protein synthesis inhibition in the mouse brain during status epilepticus. Biochem J 2006; 397: 187–94.
Chen J, Martin BL, Brautigan DL. Regulation of protein serine-threonine phosphatase type-2A by tyrosine phosphorylation. Science 1992; 257: 1261–4.
Chen J, Zheng G, Guo H, Shi ZN. Role of endoplasmic reticulum stress via the PERK signaling pathway in brain injury from status epilepticus. J Mol Neurosci 2014; 53: 677–83.
Chen X, Wu J, Hua D, Shu K, Wang JZ, Li L, et al. The c-Jun N-terminal kinase inhibitor SP600125 is neuroprotective in amygdala kindled rats. Brain Res 2010; 1357: 104–14.
Chin J, Scharfman HE. Shared cognitive and behavioral impairments in epilepsy and Alzheimer's disease and potential underlying mechanisms. Epilepsy Behav 2013; 26: 343–51.
Cleary JP, Walsh DM, Hofmeister JJ, Shankar GM, Kuskowski MA, Selkoe DJ, et al. Natural oligomers of the amyloid-beta protein specifically disrupt cognitive function. Nat Neurosci 2005; 8: 79–84.
Crespo-Biel N, Canudas AM, Camins A, Pallas M. Kainate induces AKT, ERK and cdk5/GSK3beta pathway deregulation, phosphorylates tau protein in mouse hippocampus. Neurochem Int 2007; 50: 435–42.
Croft CL, Moore BD, Ran Y, Chakrabarty P, Levites Y, Golde TE, et al. Novel monoclonal antibodies targeting the microtubule-binding domain of human tau. PLoS One 2018; 13: e0195211.
Cummings J, Lee G, Ritter A, Zhong K. Alzheimer's disease drug development pipeline: 2018. Alzheimers Dement 2018; 4: 195–214.
Dabbs K, Becker T, Jones J, Rutecki P, Seidenberg M, Hermann B. Brain structure and aging in chronic temporal lobe epilepsy. Epilepsia 2012; 53: 1033–43.
Devi L, Ohno M. PERK mediates eIF2alpha phosphorylation responsible for BACE1 elevation, CREB dysfunction and neurodegeneration in a mouse model of Alzheimer's disease. Neurobiol Aging 2014; 35: 2272–81.
DeVos SL, Goncharoff DK, Chen G, Kebodeaux CS, Yamada K, Stewart FR, et al. Antisense reduction of tau in adult mice protects against seizures. J Neurosci 2013; 33: 12887–97.
Di J, Cohen LS, Corbo CP, Phillips GR, El Idrissi A, Alonso AD. Abnormal tau induces cognitive impairment through two different mechanisms: synaptic dysfunction and neuronal loss. Sci Rep 2016; 6: 20833.
Di Nardo A, Kramvis I, Cho N, Sadowski A, Meikle L, Kwiatkowski DJ, et al. Tuberous sclerosis complex activity is required to control neuronal stress responses in an mTOR-dependent manner. J Neurosci 2009; 29: 5926–37.
Elverman KH, Resch ZJ, Quasney EE, Sabsevitz DS, Binder JR, Swanson SJ. Temporal lobe epilepsy is associated with distinct cognitive phenotypes. Epilepsy Behav 2019; 96: 61–8.
Espindola SL, Damianich A, Alvarez RJ, Sartor M, Belforte JE, Ferrario JE, et al. Modulation of tau isoforms imbalance precludes tau pathology and cognitive decline in a mouse model of tauopathy. Cell Rep 2018; 23: 709–15.
Gelinas JN, Khodagholy D, Thesen T, Devinsky O, Buzsaki G. Interictal epileptiform discharges induce hippocampal-cortical coupling in temporal lobe epilepsy. Nat Med 2016; 22: 641–8.
Gheyara AL, Ponnusamy R, Djukic B, Craft RJ, Ho K, Guo W, et al. Tau reduction prevents disease in a mouse model of Dravet syndrome. Ann Neurol 2014; 76: 443–56.
Goto J, Talos DM, Klein P, Qin W, Chekaluk YI, Anderl S, et al. Regulable neural progenitor-specific Tsc1 loss yields giant cells with organellar dysfunction in a model of tuberous sclerosis complex. Proc Natl Acad Sci U S A 2011; 108: E1070–9.
Gourmaud S, Paquet C, Dumurgier J, Pace C, Bouras C, Gray F, et al. Increased levels of cerebrospinal fluid JNK3 associated with amyloid pathology: links to cognitive decline. J Psychiatry Neurosci 2015; 40: 151–61.
Hara M, Hirokawa K, Kamei S, Uchihara T. Isoform transition from four-repeat to three-repeat tau underlies dendrosomatic and regional progression of neurofibrillary pathology. Acta Neuropathol 2013; 125: 565–79.
Hermann BP, Seidenberg M, Dow C, Jones J, Rutecki P, Bhattacharya A, et al. Cognitive prognosis in chronic temporal lobe epilepsy. Ann Neurol 2006; 60: 80–7.
Hernandez-Ronquillo L, Buckley S, Ladino LD, Wu A, Moien-Afshari F, Rizvi SA, et al. How many adults with temporal epilepsy have a mild course and do not require epilepsy surgery? Epileptic Disord 2016; 18: 137–47.
Hilbich C, Monning U, Grund C, Masters CL, Beyreuther K. Amyloid-like properties of peptides flanking the epitope of amyloid precursor protein-specific monoclonal antibody 22C11. J Biol Chem 1993; 268: 26571–7.
Hoe HS, Fu Z, Makarova A, Lee JY, Lu C, Feng L, et al. The effects of amyloid precursor protein on postsynaptic composition and activity. J Biol Chem 2009; 284: 8495–506.
Holth JK, Bomben VC, Reed JG, Inoue T, Younkin L, Younkin SG, et al. Tau loss attenuates neuronal network hyperexcitability in mouse and Drosophila genetic models of epilepsy. J Neurosci 2013; 33: 1651–9.
Hoozemans JJ, van Haastert ES, Nijholt DA, Rozemuller AJ, Scheper W. Activation of the unfolded protein response is an early event in Alzheimer's and Parkinson's disease. Neurodegener Dis 2012; 10: 212–5.
Hornberger TA, Sukhija KB, Wang XR, Chien S. mTOR is the rapamycin-sensitive kinase that confers mechanically-induced phosphorylation of the hydrophobic motif site Thr(389) in p70(S6k). FEBS Lett 2007; 581: 4562–6.
Huang X, Zhang H, Yang J, Wu J, McMahon J, Lin Y, et al. Pharmacological inhibition of the mammalian target of rapamycin pathway suppresses acquired epilepsy. Neurobiol Dis 2010; 40: 193–9.
Iijima K, Ando K, Takeda S, Satoh Y, Seki T, Itohara S, et al. Neuron-specific phosphorylation of Alzheimer's beta-amyloid precursor protein by cyclin-dependent kinase 5. J Neurochem 2000; 75: 1085–91.
Ip YT, Davis RJ. Signal transduction by the c-Jun N-terminal kinase (JNK): from inflammation to development. Curr Opin Cell Biol 1998; 10: 205–19.
Iqbal K, Alonso Adel C, Chen S, Chohan MO, El-Akkad E, Gong CX, et al. Tau pathology in Alzheimer disease and other tauopathies. Biochim Biophys Acta 2005; 1739: 198–210.
Iyer A, Prabowo A, Anink J, Spliet WG, van Rijen PC, Aronica E. Cell injury and premature neurodegeneration in focal malformations of cortical development. Brain Pathol 2014; 24: 1–17.
Jang SS, Royston SE, Lee G, Wang S, Chung HJ. Seizure-Induced Regulations of Amyloid-beta, STEP61, and STEP61 substrates involved in hippocampal synaptic plasticity. Neural Plast 2016; 2016: 2123748.
Jensen FE. Epilepsy as a spectrum disorder: Implications from novel clinical and basic neuroscience. Epilepsia 2011; 52: 1–6.
Jones NC, Nguyen T, Corcoran NM, Velakoulis D, Chen T, Grundy R, et al. Targeting hyperphosphorylated tau with sodium selenate suppresses seizures in rodent models. Neurobiol Dis 2012; 45: 897–901.
Joutsa J, Rinne JO, Hermann B, Karrasch M, Anttinen A, Shinnar S, et al. Association between childhood-onset epilepsy and amyloid burden 5 decades later. JAMA Neurol 2017; 74: 583–90.
Kirouac L, Rajic AJ, Cribbs DH, Padmanabhan J. Activation of Ras-ERK Signaling and GSK-3 by Amyloid precursor protein and

amyloid beta facilitates neurodegeneration in Alzheimer's disease. eNeuro 2017; 4: 1–21.
Kleen JK, Scott RC, Holmes GL, Roberts DW, Rundle MM, Testorf M, et al. Hippocampal interictal epileptiform activity disrupts cognition in humans. Neurology 2013; 81: 18–24.
Kodam A, Ourdev D, Maulik M, Hariharakrishnan J, Banerjee M, Wang Y, et al. A role for astrocyte-derived amyloid beta peptides in the degeneration of neurons in an animal model of temporal lobe epilepsy. Brain Pathol 2019; 29: 28–44.
Kunkle BW, Grenier-Boley B, Sims R, Bis JC, Damotte V, Naj AC, et al. Genetic meta-analysis of diagnosed Alzheimer's disease identifies new risk loci and implicates Abeta, tau, immunity and lipid processing. Nat Genet 2019; 51: 414–30.
Kurz A, Perneczky R. Amyloid clearance as a treatment target against Alzheimer's disease. J Alzheimers Dis 2011; 24: 61–73.
Lalonde R, Dumont M, Staufenbiel M, Strazielle C. Neurobehavioral characterization of APP23 transgenic mice with the SHIRPA primary screen. Behav Brain Res 2005; 157: 91–8.
Lam AD, Deck G, Goldman A, Eskandar EN, Noebels J, Cole AJ. Silent hippocampal seizures and spikes identified by foramen ovale electrodes in Alzheimer's disease. Nat Med 2017; 23: 678–80.
Lee KJ, Moussa CE, Lee Y, Sung Y, Howell BW, Turner RS, et al. Beta amyloid-independent role of amyloid precursor protein in generation and maintenance of dendritic spines. Neuroscience 2010; 169: 344–56.
Lee MS, Kao SC, Lemere CA, Xia W, Tseng HC, Zhou Y, et al. APP processing is regulated by cytoplasmic phosphorylation. J Cell Biol 2003; 163: 83–95.
Lesne S, Koh MT, Kotilinek L, Kayed R, Glabe CG, Yang A, et al. A specific amyloid-beta protein assembly in the brain impairs memory. Nature 2006; 440: 352–7.
Li Z, Hall AM, Kelinske M, Roberson ED. Seizure resistance without parkinsonism in aged mice after tau reduction. Neurobiol Aging 2014; 35: 2617–24.
Liang Z, Liu F, Iqbal K, Grundke-Iqbal I, Gong CX. Dysregulation of tau phosphorylation in mouse brain during excitotoxic damage. J Alzheimers Dis 2009; 17: 531–9.
Lippman-Bell JJ, Rakhade SN, Klein PM, Obeid M, Jackson MC, Joseph A, et al. AMPA receptor antagonist NBQX attenuates later-life epileptic seizures and autistic-like social deficits following neonatal seizures. Epilepsia 2013; 54: 1922–32.
Liu G, Guo H, Guo C, Zhao S, Gong D, Zhao Y. Involvement of IRE1alpha signaling in the hippocampus in patients with mesial temporal lobe epilepsy. Brain Res Bull 2011; 84: 94–102.
Liu SJ, Zheng P, Wright DK, Dezsi G, Braine E, Nguyen T, et al. Sodium selenate retards epileptogenesis in acquired epilepsy models reversing changes in protein phosphatase 2A and hyperphosphorylated tau. Brain 2016; 139: 1919–38.
Mackenzie IR, Miller LA. Senile plaques in temporal lobe epilepsy. Acta Neuropathol 1994; 87: 504–10.
Martin L, Latypova X, Wilson CM, Magnaudeix A, Perrin ML, Terro F. Tau protein phosphatases in Alzheimer's disease: the leading role of PP2A. Ageing Res Rev 2013; 12: 39–49.
McKhann GM, Knopman DS, Chertkow H, Hyman BT, Jack CR Jr, Kawas CH, et al. The diagnosis of dementia due to Alzheimer's disease: recommendations from the National Institute on Aging-Alzheimer's Association workgroups on diagnostic guidelines for Alzheimer's disease. Alzheimers Dement 2011; 7: 263–9.
Miners JS, Van Helmond Z, Chalmers K, Wilcock G, Love S, Kehoe PG. Decreased expression and activity of neprilysin in Alzheimer disease are associated with cerebral amyloid angiopathy. J Neuropathol Exp Neurol 2006; 65: 1012–21.
Moechars D, Dewachter I, Lorent K, Reverse D, Baekelandt V, Naidu A, et al. Early phenotypic changes in transgenic mice that overexpress different mutants of amyloid precursor protein in brain. J Biol Chem 1999; 274: 6483–92.
Morales-Corraliza J, Mazzella MJ, Berger JD, Diaz NS, Choi JH, Levy E, et al. In vivo turnover of tau and APP metabolites in the brains of wild-type and Tg2576 mice: greater stability of sAPP in the beta-amyloid depositing mice. PLoS One 2009; 4: e7134.
Moreno JA, Radford H, Peretti D, Steinert JR, Verity N, Martin MG, et al. Sustained translational repression by eIF2alpha-P mediates prion neurodegeneration. Nature 2012; 485: 507–11.
Mucke L, Masliah E, Yu GQ, Mallory M, Rockenstein EM, Tatsuno G, et al. High-level neuronal expression of abeta 1-42 in wild-type human amyloid protein precursor transgenic mice: synaptotoxicity without plaque formation. J Neurosci 2000; 20: 4050–8.
Noebels J. A perfect storm: Converging paths of epilepsy and Alzheimer's dementia intersect in the hippocampal formation. Epilepsia 2011; 52: 39–46.
O'Brien RJ, Wong PC. Amyloid precursor protein processing and Alzheimer's disease. Annu Rev Neurosci 2011; 34: 185–204.
O'Connor T, Sadleir KR, Maus E, Velliquette RA, Zhao J, Cole SL, et al. Phosphorylation of the translation initiation factor eIF2alpha increases BACE1 levels and promotes amyloidogenesis. Neuron 2008; 60: 988–1009.
Osler M, Mortensen EL, Christensen K, Christensen GT. A bidirectional association between cognitive ability in young adulthood and epilepsy: a population-based cohort study. Int J Epidemiol 2018; 47: 1151–8.
Palop JJ, Chin J, Roberson ED, Wang J, Thwin MT, Bien-Ly N, et al. Aberrant excitatory neuronal activity and compensatory remodeling of inhibitory hippocampal circuits in mouse models of Alzheimer's disease. Neuron 2007; 55: 697–711.
Palop JJ, Mucke L. Epilepsy and cognitive impairments in Alzheimer disease. Arch Neurol 2009; 66: 435–40.
Pardoe HR, Cole JH, Blackmon K, Thesen T, Kuzniecky R, Human Epilepsy Project I. Structural brain changes in medically refractory focal epilepsy resemble premature brain aging. Epilepsy Res 2017; 133: 28–32.
Pasciuto E, Ahmed T, Wahle T, Gardoni F, D'Andrea L, Pacini L, et al. Dysregulated ADAM10-mediated processing of APP during a critical time window leads to synaptic deficits in fragile X syndrome. Neuron 2015; 87: 382–98.
Patrick GN, Zukerberg L, Nikolic M, de la Monte S, Dikkes P, Tsai LH. Conversion of p35 to p25 deregulates Cdk5 activity and promotes neurodegeneration. Nature 1999; 402: 615–22.
Pei JJ, An WL, Zhou XW, Nishimura T, Norberg J, Benedikz E, et al. P70 S6 kinase mediates tau phosphorylation and synthesis. FEBS Lett 2006; 580: 107–14.
Perez SE, Miguel JC, He B, Malek-Ahmadi M, Abrahamson EE, Ikonomovic MD, et al. Frontal cortex and striatal cellular and molecular pathobiology in individuals with Down syndrome with and without dementia. Acta Neuropathol 2019; 137: 413–36.
Prabowo AS, Iyer AM, Veersema TJ, Anink JJ, Schouten-van Meeteren AY, Spliet WG, et al. Expression of neurodegenerative disease-related proteins and caspase-3 in glioneuronal tumours. Neuropathol Appl Neurobiol 2015; 41: e1–15.
Puvenna V, Engeler M, Banjara M, Brennan C, Schreiber P, Dadas A, et al. Is phosphorylated tau unique to chronic traumatic encephalopathy? Phosphorylated tau in epileptic brain and chronic traumatic encephalopathy. Brain Res 2016; 1630: 225–40.
Rakhade SN, Zhou C, Aujla PK, Fishman R, Sucher NJ, Jensen FE. Early alterations of AMPA receptors mediate synaptic potentiation induced by neonatal seizures. J Neurosci 2008; 28: 7979–90.
Roberson ED, Halabisky B, Yoo JW, Yao J, Chin J, Yan F, et al. Amyloid-beta/Fyn-induced synaptic, network, and cognitive impairments depend on tau levels in multiple mouse models of Alzheimer's disease. J Neurosci 2011; 31: 700–11.
Schoch KM, DeVos SL, Miller RL, Chun SJ, Norrbom M, Wozniak DF, et al. Increased 4R-tau induces pathological changes in a human-tau mouse model. Neuron 2016; 90: 941–7.
Sheng JG, Boop FA, Mrak RE, Griffin WS. Increased neuronal beta-amyloid precursor protein expression in human temporal lobe epilepsy: association with interleukin-1 alpha immunoreactivity. J Neurochem 1994; 63: 1872–9.

Sima X, Xu J, Li J, Zhong W, You C. Expression of beta-amyloid precursor protein in refractory epilepsy. Mol Med Rep 2014; 9: 1242–8.

Sjogren M, Davidsson P, Tullberg M, Minthon L, Wallin A, Wikkelso C, et al. Both total and phosphorylated tau are increased in Alzheimer's disease. J Neurol Neurosurg Psychiatry 2001; 70: 624–30.

Spigolon G, Veronesi C, Bonny C, Vercelli A. c-Jun N-terminal kinase signaling pathway in excitotoxic cell death following kainic acid-induced status epilepticus. Eur J Neurosci 2010; 31: 1261–72.

Standen CL, Brownlees J, Grierson AJ, Kesavapany S, Lau KF, McLoughlin DM, et al. Phosphorylation of thr(668) in the cytoplasmic domain of the Alzheimer's disease amyloid precursor protein by stress-activated protein kinase 1b (Jun N-terminal kinase-3). J Neurochem 2001; 76: 316–20.

Sun YX, Ji X, Mao X, Xie L, Jia J, Galvan V, et al. Differential activation of mTOR complex 1 signaling in human brain with mild to severe Alzheimer's disease. J Alzheimers Dis 2014; 38: 437–44.

Tai TY, Warner LN, Jones TD, Jung S, Concepcion FA, Skyrud DW, et al. Antiepileptic action of c-Jun N-terminal kinase (JNK) inhibition in an animal model of temporal lobe epilepsy. Neuroscience 2017; 349: 35–47.

Tai XY, Koepp M, Duncan JS, Fox N, Thompson P, Baxendale S, et al. Hyperphosphorylated tau in patients with refractory epilepsy correlates with cognitive decline: a study of temporal lobe resections. Brain 2016; 139: 2441–55.

Talos DM, Jacobs LM, Gourmaud S, Coto CA, Sun H, Lim KC, et al. Mechanistic target of rapamycin complex 1 and 2 in human temporal lobe epilepsy. Ann Neurol 2018; 83: 311–27.

Talos DM, Sun H, Zhou X, Fitzgerald EC, Jackson MC, Klein PM, et al. The interaction between early life epilepsy and autistic-like behavioral consequences: a role for the mammalian target of rapamycin (mTOR) pathway. PLoS One 2012; 7: e35885.

Tamagno E, Guglielmotto M, Monteleone D, Vercelli A, Tabaton M. Transcriptional and post-transcriptional regulation of beta-secretase. IUBMB Life 2012; 64: 943–50.

Tang Z, Ioja E, Bereczki E, Hultenby K, Li C, Guan Z, et al. mTor mediates tau localization and secretion: Implication for Alzheimer's disease. Biochim Biophys Acta 2015; 1853: 1646–57.

Taylor J, Kolamunnage-Dona R, Marson AG, Smith PE, Aldenkamp AP, Baker GA, et al. Patients with epilepsy: cognitively compromised before the start of antiepileptic drug treatment? Epilepsia 2010; 51: 48–56.

Tellechea P, Pujol N, Esteve-Belloch P, Echeveste B, Garcia-Eulate MR, Arbizu J, et al. Early- and late-onset Alzheimer disease: are they the same entity? Neurologia 2018; 33: 244–53.

Tellez-Zenteno JF, Hernandez-Ronquillo L. A review of the epidemiology of temporal lobe epilepsy. Epilepsy Res Treat 2012; 2012: 630853.

Thom M, Liu JY, Thompson P, Phadke R, Narkiewicz M, Martinian L, et al. Neurofibrillary tangle pathology and Braak staging in chronic epilepsy in relation to traumatic brain injury and hippocampal sclerosis: a post-mortem study. Brain 2011; 134: 2969–81.

Tian FF, Zeng C, Ma YF, Guo TH, Chen JM, Chen Y, et al. Potential roles of Cdk5/p35 and tau protein in hippocampal mossy fiber sprouting in the PTZ kindling model. Clin Lab 2010; 56: 127–36.

Torres-Peraza JF, Engel T, Martin-Ibanez R, Sanz-Rodriguez A, Fernandez-Fernandez MR, Esgleas M, et al. Protective neuronal induction of ATF5 in endoplasmic reticulum stress induced by status epilepticus. Brain 2013; 136: 1161–76.

Tumani H, Jobs C, Brettschneider J, Hoppner AC, Kerling F, Fauser S. Effect of epileptic seizures on the cerebrospinal fluid: a systematic retrospective analysis. Epilepsy Res 2015; 114: 23–31.

Ung H, Cazares C, Nanivadekar A, Kini L, Wagenaar J, Becker D, et al. Interictal epileptiform activity outside the seizure onset zone impacts cognition. Brain 2017; 140: 2157–68.

van Vliet EA, Forte G, Holtman L, den Burger JC, Sinjewel A, de Vries HE, et al. Inhibition of mammalian target of rapamycin reduces epileptogenesis and blood-brain barrier leakage but not microglia activation. Epilepsia 2012; 53: 1254–63.

Vossel KA, Ranasinghe KG, Beagle AJ, Mizuiri D, Honma SM, Dowling AF, et al. Incidence and impact of subclinical epileptiform activity in Alzheimer's disease. Ann Neurol 2016; 80: 858–70.

Vossel KA, Tartaglia MC, Nygaard HB, Zeman AZ, Miller BL. Epileptic activity in Alzheimer's disease: causes and clinical relevance. Lancet Neurol 2017; 16: 311–22.

Wang JZ, Xia YY, Grundke-Iqbal I, Iqbal K. Abnormal hyperphosphorylation of tau: sites, regulation, and molecular mechanism of neurofibrillary degeneration. J Alzheimers Dis 2013; 33: S123–39.

Westmark CJ. What's hAPPening at synapses? The role of amyloid beta-protein precursor and beta-amyloid in neurological disorders. Mol Psychiatry 2013; 18: 425–34.

Westmark CJ, Chuang SC, Hays SA, Filon MJ, Ray BC, Westmark PR, et al. APP Causes Hyperexcitability in Fragile X Mice. Front Mol Neurosci 2016; 9: 147.

Westmark CJ, Malter JS. FMRP mediates mGluR5-dependent translation of amyloid precursor protein. PLoS Biol 2007; 5: e52.

Westmark CJ, Westmark PR, Beard AM, Hildebrandt SM, Malter JS. Seizure susceptibility and mortality in mice that over-express amyloid precursor protein. Int J Clin Exp Pathol 2008; 1: 157–68.

Witt JA, Helmstaedter C. Should cognition be screened in new-onset epilepsies? A study in 247 untreated patients. J Neurol 2012; 259: 1727–31.

Yamamoto A, Murphy N, Schindler CK, So NK, Stohr S, Taki W, et al. Endoplasmic reticulum stress and apoptosis signaling in human temporal lobe epilepsy. J Neuropathol Exp Neurol 2006; 65: 217–25.

Yan R. Physiological Functions of the beta-Site Amyloid Precursor Protein Cleaving Enzyme 1 and 2. Front Mol Neurosci 2017; 10: 97.

Yan XX, Cai Y, Shelton J, Deng SH, Luo XG, Oddo S, et al. Chronic temporal lobe epilepsy is associated with enhanced Alzheimer-like neuropathology in 3xTg-AD mice. PLoS One 2012; 7: e48782.

Youmans KL, Tai LM, Kanekiyo T, Stine WB Jr, Michon SC, Nwabuisi-Heath E, et al. Intraneuronal Abeta detection in 5xFAD mice by a new Abeta-specific antibody. Mol Neurodegener 2012; 7: 8.

Zeng LH, Rensing NR, Wong M. The mammalian target of rapamycin signaling pathway mediates epileptogenesis in a model of temporal lobe epilepsy. J Neurosci 2009; 29: 6964–72.

Zhao X, Kotilinek LA, Smith B, Hlynialuk C, Zahs K, Ramsden M, et al. Caspase-2 cleavage of tau reversibly impairs memory. Nat Med 2016; 22: 1268–76.

Ziyatdinova S, Gurevicius K, Kutchiashvili N, Bolkvadze T, Nissinen J, Tanila H, et al. Spontaneous epileptiform discharges in a mouse model of Alzheimer's disease are suppressed by antiepileptic drugs that block sodium channels. Epilepsy Res 2011; 94: 75–85.